


Timing of the Middle-to-Upper Palaeolithic transition in the Iberian inland (Cardina-Salto do Boi, Côa Valley, Portugal)

Thierry Aubry^{a,b,*} , Luca Antonio Dimuccio^{b,c}, António Fernando Barbosa^a, Luís Luís^{a,b}, André Tomás Santos^{a,b}, Marcelo Silvestre^a, Kristina Jørkov Thomsen^d, Eike Rades^{d,e}, Martin Autzen^d, Andrew Sean Murray^e

^aCôa Parque, Fundação para a Salvaguarda e Valorização do Vale do Côa. Rua do Museu, 5150-610 Vila Nova de Foz Côa, Portugal

^bUNIARQ—Centro de Arqueologia Universidade de Lisboa, Faculdade de Letras, Alameda da Universidade, 1600-214 Lisboa, Portugal

^cUniversity of Coimbra, Centre of Studies in Geography and Spatial Planning (CEGOT), FLUC, Department of Geography and Tourism, Largo da Porta Férea, 3004-530 Coimbra, Portugal

^dCenter for Nuclear Technologies, Technical University of Denmark, DTU Risø Campus, Denmark

^eNordic Laboratory for Luminescence Dating, Department of Geoscience, Aarhus University, Risø Campus, Denmark

*Corresponding author at: Côa Parque, Fundação para a Salvaguarda e Valorização do Vale do Côa, Rua do Museu, 5150-610 Vila Nova de Foz Côa, Portugal.
E-mail address: thaubry@sapo.pt.

(RECEIVED June 16, 2019; ACCEPTED April 24, 2020)

Abstract

The timing of the Neanderthal-associated Middle Palaeolithic demise and a possible overlap with anatomically modern humans (AMH) in some regions of Eurasia continues to be debated. The Iberian Peninsula is considered a possible refuge zone for the last Neanderthals, but the chronology of the later Middle Palaeolithic record has undergone revision and has increased the debate on the timing of Neanderthal extinction. Here we report on a study of the 5-m-thick archaeological stratigraphy of the Cardina-Salto do Boi, an open-air site located in inland Iberia, from which optically stimulated luminescence (OSL) ages were obtained for Middle and Upper Palaeolithic occupations preserved in overbank alluvial deposits. Geomorphology, archaeostratigraphy, stone-tool evolution, and OSL dating support the persistence of Neanderthals after 41 ka in central Iberia; the transition between the Middle Palaeolithic material culture and the AMH-associated Aurignacian blade and bladelet production is estimated to lie between 34.0 ± 2.0 ka and 38.4 ± 1.9 ka. Our results demonstrate that investigations focusing on different geomorphological situations are necessary to overcome the current limitations of the evidence and to establish more consistent models for Neanderthal disappearance and AMH expansion in the Iberian Peninsula.

Keywords: Neanderthal; Modern Human; Middle-to-Upper Palaeolithic; Iberia

INTRODUCTION

Since the end of the 1980s, based on ages under 40,000 ¹⁴C yr BP, it has been widely accepted that southern Iberia represents a possible refuge zone for the last Neanderthal population (Hublin et al., 1995; Zilhão, 2000) and that this population persisted until approximately 37,000 cal yr BP (Zilhão, 2006a; Zilhão et al., 2010), or even as late as ~28,000 cal yr BP (Straus et al., 2000; Finlayson et al., 2006). This hypothesis implies coexistence for several millennia with anatomically modern humans (AMH), who lived in northern Iberia from around 42,000 cal yr BP (Wood et al., 2014; Hublin, 2017). It also implies the

existence of a biogeographical frontier along the Ebro Basin, which would have functioned as a barrier to migration and diffusion between Neanderthals and AMH (Zilhão, 2000).

However, new radiocarbon data from several key Late Middle Palaeolithic European sites (Higham et al., 2014) and direct radiocarbon dating of Neanderthal remains (Devièse et al., 2017) using refined sample pre-treatment measures and suitable sample selection have pushed back some of the youngest radiocarbon ages for the Middle Palaeolithic to about 42,000 cal yr BP. The Iberian Peninsula, the westernmost part of Europe, has been subject to special attention in this research. The associations between dates from Gorham's Cave and their supposed archaeological contexts (Fig. 1; Zilhão and Pettitt, 2006) have been questioned, and the dates from El Salt, Jarama VI, and Zafarraya have been pushed back several millennia (see Fig. 1; Maroto et al., 2012; Kehl et al., 2013; Wood et al., 2013; Galván et al., 2014).

Cite this article: Aubry, T. et al 2020. Timing of the Middle-to-Upper Palaeolithic transition in the Iberian inland (Cardina-Salto do Boi, Côa Valley, Portugal). *Quaternary Research* 1–21. <https://doi.org/10.1017/qua.2020.43>



Figure 1. (color online) Locations of Middle Palaeolithic and Aurignacian sites in the Iberian Peninsula and sites mentioned in the text.

Nevertheless, the hypothesis of a persistent Neanderthal presence in southern Iberia has not been invalidated; there remains evidence for a relatively late survival of Neanderthals (Zilhão et al., 2017, Carrión et al., 2019), and more work is needed.

The current discussion on the Middle-to-Upper Palaeolithic transition in Iberia shows clear shortcomings resulting directly from: (1) the lack of research in inland Iberia, when compared to the coastal regions; (2) the difficulties of locating open-air sites that can expand the geographic and temporal scope of the archaeological record; and (3) the challenges of dating (especially using ^{14}C) (Aubry et al., 2002; Alcaraz-Castaño, 2015).

Our view of the importance of the open-air Cardina-Salto do Boi site discussed in this paper is based on the above discussion. The site is located in Northeastern Portugal along the Côa River (see Fig. 1), halfway between the central Portuguese and Asturias site clusters of Middle and Upper Palaeolithic occupations. The site also presents a sequence of deposits containing artefacts from the Middle Palaeolithic through to the Upper Palaeolithic. These deposits have the potential to provide an important new contribution to the ongoing debate concerning the chronological overlap between Neanderthal and AMH populations in Western Eurasia and the geographical and palaeoenvironmental context of such overlap.

CARDINA-SALTO DO BOI SITE

The Côa River is a Portuguese left-bank tributary of the Douro River, one of the major watercourses that cross the northwest Iberian Mountains from east to west (see Fig. 1). The 120-km-long river basin is controlled by the tectonic structure of the south-southwest/north-northeast Manteigas-Vilariça-Bragança fault system, separating the basin from the Portuguese Western Mountains (Ferreira, 1978; Aubry et al., 2012a). The Côa River basin comprises two different geological sectors. Upstream, the river flows in a deeply gorged valley through Hercynian granites (Silva and Ribeiro, 1991). The last 17 km of the Côa, before the confluence with the Douro, grades to a meandering pattern in intensely folded and faulted metasedimentary rocks (phyllite, greywacke, and quartzite), ranging in age from the Precambrian to the Ordovician (Silva and Ribeiro, 1991).

The last 22 km of the Côa River valley and its confluence with the Douro are well known as having the largest concentration of preserved open-air Palaeolithic rock art, and the area was classified as a UNESCO World Heritage site in 1998 (Zilhão, 1997). Since 1995, 22 open-air sites have been identified in an area of less than 400 km², along the river's last 9 km (Fig. 2). These lie in a region where Upper Palaeolithic settlement was previously unknown, and their existence partially contradicts the accepted logistic hunting sites model for the Iberian inland's scarce occurrences

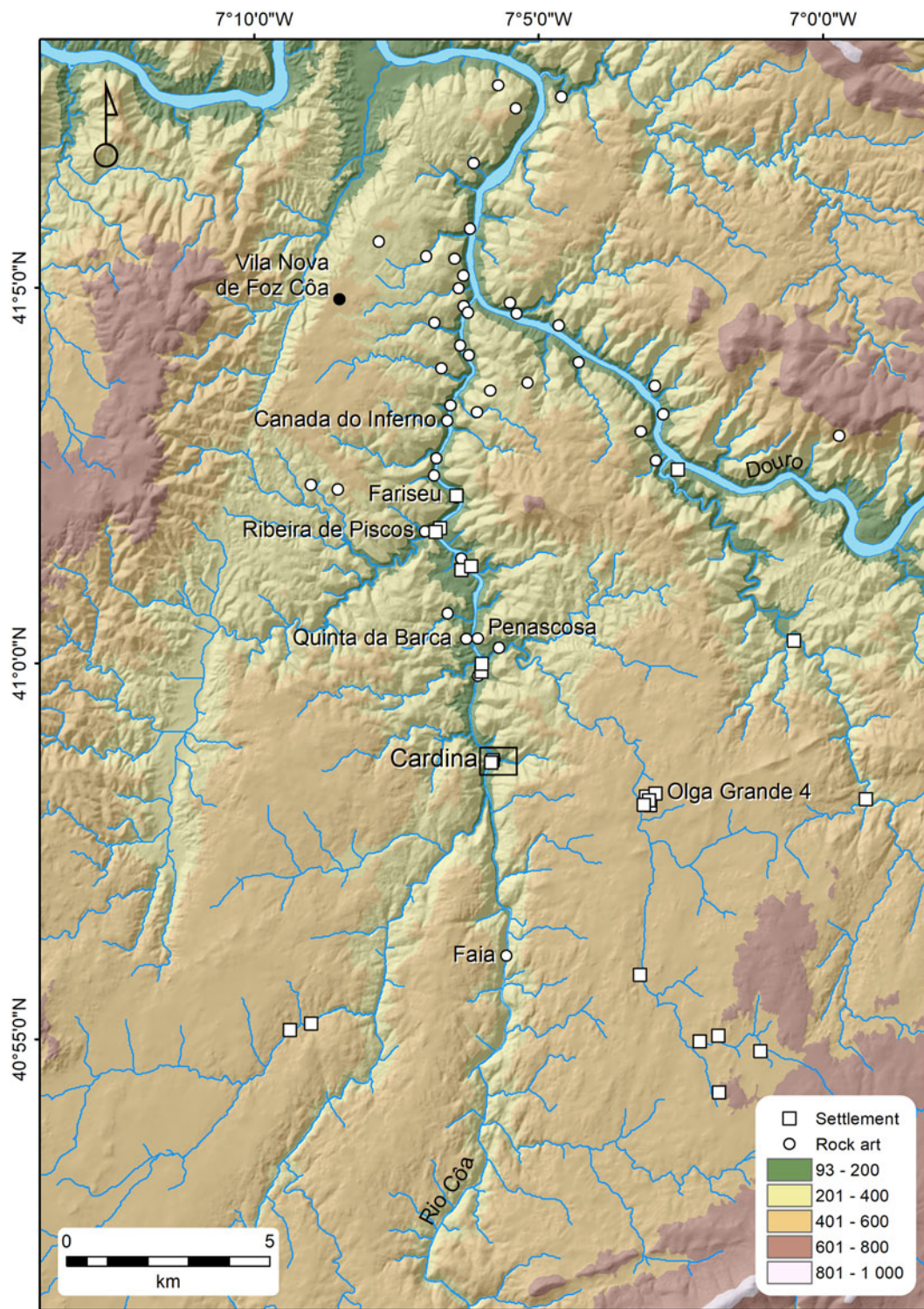


Figure 2. (color online) Location map of the Palaeolithic sites in the Côa Valley.

(Davidson, 1986). The sites are found both on the valley bottom and on the surrounding granite plateau, along the eastern limit of the northern Meseta (Zilhão et al., 1995; Aubry et al., 2002; Aubry, 2009).

A relative chronology for the Côa Valley Upper Palaeolithic settlement phases was established from the stratigraphic sequences identified at the sites using a geoarchaeological

approach (Aubry et al., 2010). Thermoluminescence (TL) ages were obtained from heated quartz and quartzite pebbles and optically stimulated luminescence (OSL) ages were obtained from sediments at Cardina, Olga Grande 4, Quinta da Barca Sul, and Fariseu (see Fig. 2; Valladas et al., 2001; Mercier et al., 2006; Aubry et al., 2010). From a radiocarbon perspective, the acid soils developed on schist and granite do

not favour the preservation of macro-organic remains. However, bones and teeth fragments were recovered in stratigraphic level 4 of Fariseu (Aubry, 2009). The nitrogen (N) content tested on Cardina-Salto do Boi faunal remains from Gravettian layers has revealed that collagen is not sufficiently preserved to be used for radiocarbon ages (Monge Soares, A., personal communication, 2008). However, two radiocarbon ages from the Early Holocene, 10,405–10,240 cal yr BP ($9,160 \pm 30$ ^{14}C yr BP [Beta-460528], 2σ) and 10,496–10,266 cal yr BP ($9,220 \pm 30$ yr BP [Beta-460529], 2σ), using the IntCal13 calibration curve (Reimer et al., 2013) were obtained on cremated bones from the top of layer 4 (Aubry et al., 2017); additionally, dates from the Younger Dryas stade, 12,601–12,244 cal yr BP ($10,510 \pm 40$ yr BP [Beta-213130]) and 11,759–10,781 cal yr BP ($9,830 \pm 130$ ^{14}C yr BP [Ua-32645]), were obtained from two bones from layer 4 at Fariseu (Aubry, 2009). In addition, a charcoal fragment from Fariseu's layer 9 was dated by accelerator mass spectrometry to 23,175–22,595 cal yr BP ($19,020 \pm 80$ ^{14}C yr BP [GrA-40167]), demonstrating the potential conservation of last glacial maximum macro-organic material in alluvial deposits.

Cardina-Salto do Boi was the first Upper Palaeolithic site discovered in the area, in 1995, yielding the first Côa Valley rock art context (Zilhão et al., 1995). The 1-m-thick sequence of deposits revealed by excavation between 1995 and 2001 is preserved on the top of a left-bank meander, 166 m above sea level and 20 m above the Côa riverbed level, just upstream of a rhyolite dyke (Fig. 3). Four main lithostratigraphic units were defined during this first phase of excavation (1995–2001), which did not reach bedrock. The deposits of layers 1 to 4b are interpreted as the result of slope processes initiated by surface runoff (Bergadà, 2009). The stone-tool assemblage from layers 4b and 4a can be assigned to the Late Gravettian at the bottom, then to the Solutrean, Magdalenian, Azilian, and the Pre-Boreal at the top; these associations are supported by TL (Valladas et al., 2001) and radiocarbon dates (Aubry et al., 2017). Based on ceramic fragments and flint bladelets (layer 3) and modern ceramic fragments (layers 1 and 2), the top layers contain Neolithic to Bronze Age human occupations.

A second phase of archaeological excavation began in 2014, undertaken by the PALÆCOA project, including tests in other areas, in order to define the extent of the site and to observe the entire sequence of deposits (see Fig. 3; Aubry et al., 2017). Ongoing work has revealed an open-air 5-m-thick stratigraphic succession, with remains of older human occupations. This has allowed a comprehensive archaeostratigraphic study of the site using integrated multi/pluridisciplinary analyses aimed at a reconstruction of formation processes, spatial analysis, a study of stone-tool artifacts, and dating of the archaeological/sedimentary records.

MATERIAL AND METHODS

Geoarchaeological approach

The data from the Cardina-Salto do Boi open-air archaeological site were collected using a standard geoarchaeological

approach, including a geomorphological and geological study of the site surroundings, sedimentological description, and stratigraphic correlation of the siliciclastic deposits exposed during excavation, as well as a subsequent sampling program for grain-size and clay mineralogy laboratory analyses. Fieldwork involved the systematic description of exposed cross sections and profiles to reconstruct stratigraphic events and their vertical and lateral variations.

In particular, due to the presence of a local stratigraphy with recurrent sedimentary features, the field description of the Cardina-Salto do Boi siliciclastic succession was conducted using facies analysis, which links the physical characteristics displayed by a single layer or by a set of layers to a well-defined sedimentary process (e.g., Moore, 1949; Ricci Lucchi, 1980). Therefore, to be able to use the facies concept in archaeology (see Angelucci et al., 2013), informal geoarchaeological field units (GFUs) were identified based on sedimentological (lithostratigraphical), pedological, or archaeological criteria and used as field categories. These field units were later grouped into geoarchaeological complexes based on major changes in depositional style, as well as major stratigraphic unconformities (details in Angelucci, 2002).

In order to complement the observations made in the field and to better recognise the natural sedimentary processes and the anthropogenic inputs/disturbances for the siliciclastics deposits that make up the 5-m-thick Cardina-Salto do Boi stratigraphic succession, 18 samples for grain-size analysis and clay mineralogy determination were collected during fieldwork seasons in 2018. The selection of samples focused on achieving satisfactory coverage of the different identified facies and GFUs, as shown in the cross section and in the composite stratigraphic log of Figures 4 and 5, respectively. Basically, field and laboratory sediment descriptions were made using a comprehensive form addressing the sedimentary, pedogenic, and anthropogenic characteristics of the deposits (e.g., Keeley and Macphail, 1981; FAO-Isric, 1990; Brown, 1997; Goldberg and Macphail, 2006) to assess the deposition and formation processes at the site.

Grain-size and clay mineralogy laboratory analyses

For each sample, grain-size analysis was carried out using a Horiba LA-950 laser particle-size analyser (detection range from 0.01 μm to 3000 μm). After sieving with a 2-mm mesh to separate the coarse fragments (gravel), sample pre-treatment included suspension in sodium hexametaphosphate (5 g/L) and hydrogen peroxide (35%) for 12 h, as well as ultrasonic suspension for 60 s in the analyser to achieve optimal dispersion. Full description of the methodology implemented in the laser diffraction particle-size analysis is laid out in the supplementary information of Sitzia et al. (2017).

Grain-size frequency-distribution curves obtained from laser diffraction were deconvoluted (parametric curve fitting) to identify the main modes (Qin et al., 2005). All grain-size analysis and measurements were processed at PACEA laboratory (University of Bordeaux, France).

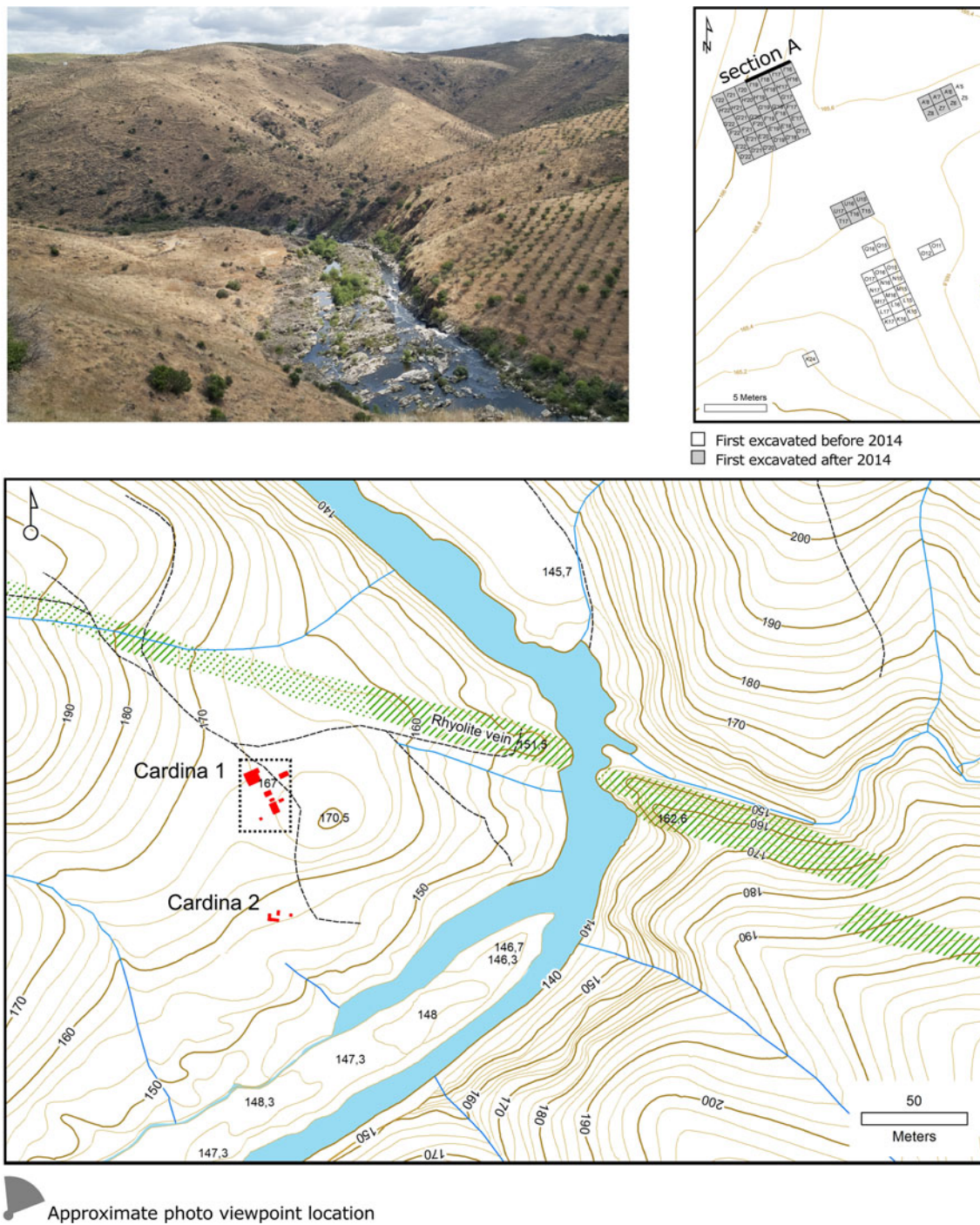


Figure 3. (color online) Topographic map and photography of the Cardina site (from southwest). Excavated area at the end of the 2018 field season and location of cross-section A in the excavation grid.

Clay mineralogy was estimated by X-ray diffraction (XRD) on the $<2 \mu\text{m}$ fraction, which was extracted by settling according to Stokes's law (Moore and Reynolds, 1997). Oriented slides of clay residue were obtained from sedimentation of clay suspensions on glass slides and run in a Malvern PANalytical X-ray diffractometer Aeris equipped with a $\text{CuK}\alpha$ X-ray tube and a detector that operate at 40 kV and 15 mA intensity (at the Earth Sciences Department of Coimbra University). Three runs were performed for each sample

to discriminate clay phases: (i) air-drying (normal run), (ii) ethylene-glycol vapour saturation for 24 h (glycol run), and (iii) heating at 550°C during 2 h (heating run), as recommended by Moore and Reynolds (1997). Continuous goniometer scans from 2° to 29° (of 2θ) were executed for normal runs and from 2° to 15° (of 2θ) for glycol and heating runs, with a step size of 0.02° (of 2θ). Clay minerals were identified using their main diffraction (d_{001}) peak and by comparing the three diffractograms obtained for each sample.

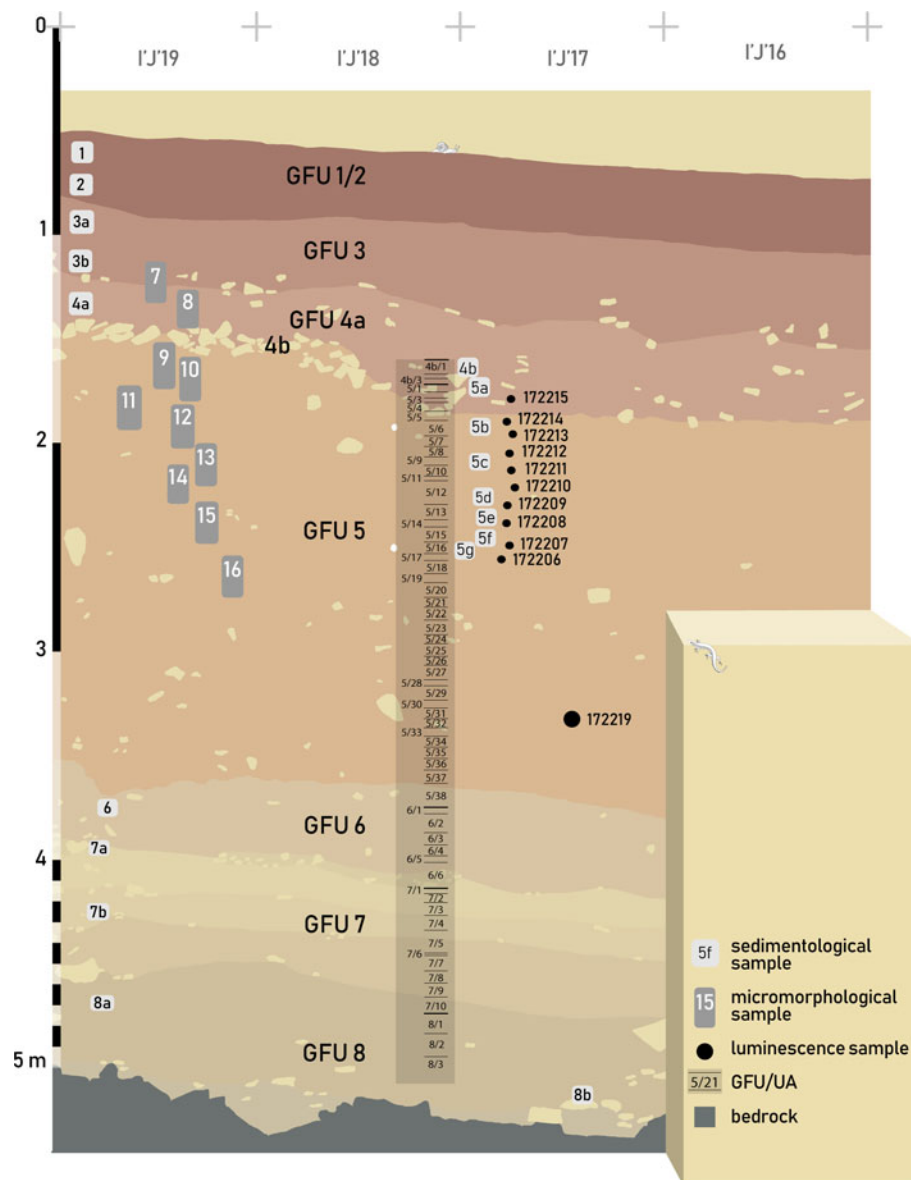


Figure 4. (color online) Stratigraphic sequence, field units, and sample locations in reference cross-section A.

Semi-quantitative abundance of clay minerals was determined through the peak areas of the basal reflection for the main clay mineral groups present on glycolated diffractograms, weighted by empirical factors. According to various authors (e.g., Moore and Reynolds, 1997; Kahle et al., 2002), this approach allows a rough estimate of actual mineral percentages.

To be able to better understand the sediment transportation pathway, the illite crystallinity and the illite chemical index were measured on the XRD diffractograms. The illite crystallinity (or Kübler index) was measured as the full width at half maximum of the illite 10Å peak (Diekmann et al., 1996; Kübler and Jaboyedoff, 2000). Generally, low values (<0.4) of illite 10Å peak width indicate good crystallinities (relatively unaltered illite), and high values (>0.8) indicate poor crystallinities (highly degraded illite). The illite chemical index (or Esquevin index) was estimated using a ratio between the 5Å and 10Å peak intensities (Esquevin, 1969;

Gingele, 1996). Values of 5Å/10Å illite peak intensities >0.5 indicate Al-rich illite, interpreted as formed under strong hydrolysis. Values of 5Å/10Å illite peak intensities <0.5 represent Fe/Mg-rich illite (biotite, mica), which is characteristic of physical erosion (Gingele, 1996).

Lithic analysis

Since 1995, all the deposits from GFUs 4 and 5 have been excavated according to lithostratigraphic units combined with 5-cm-thick artificial units (UAs), used to constrain the horizontal and vertical position of non-piece-plotted artifacts or materials recovered by water sieving with 2-mm grids. From the top to bottom of each GFU, the 5-cm-thick units are numbered sequentially per quarter of each square-meter unit of the excavation grid. Stone fragments larger than 5 cm recovered in layers 4a and 4b (GFU 4), as well as in

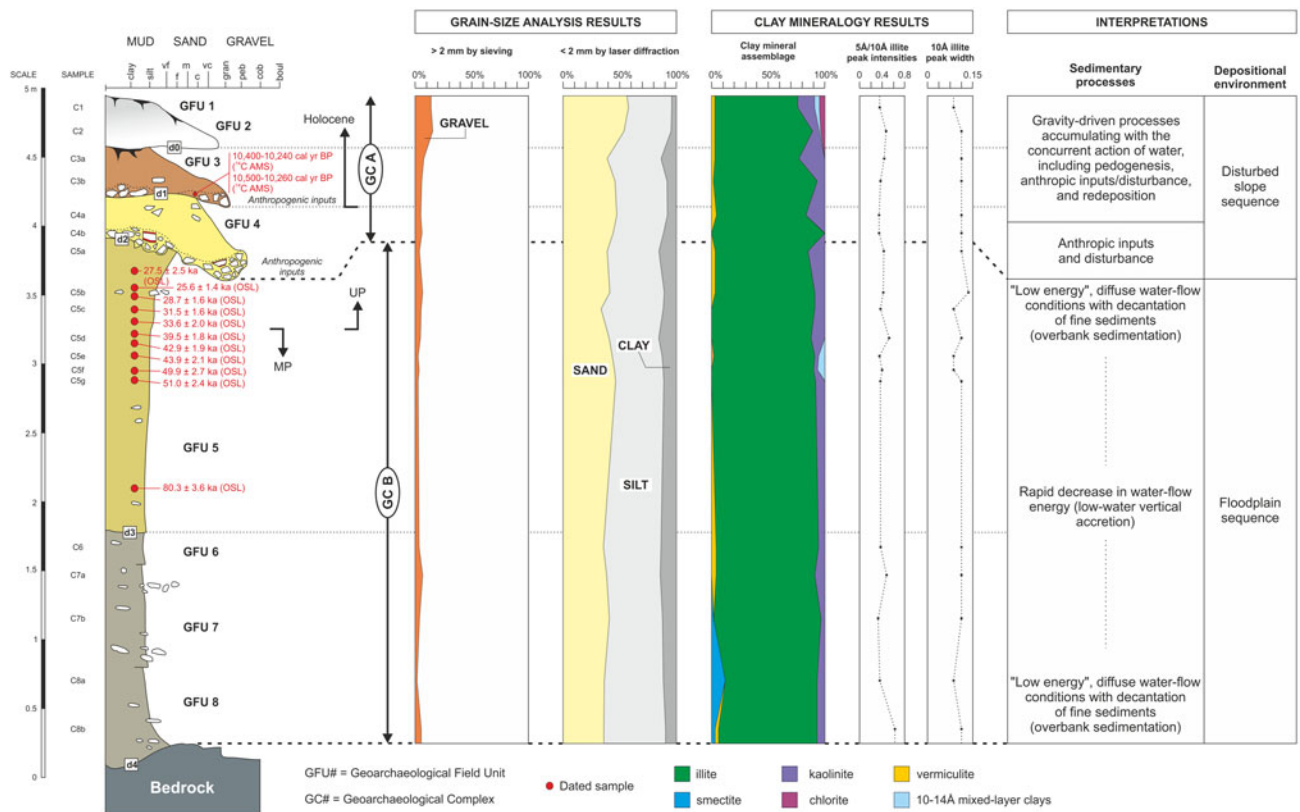


Figure 5. (color online) Cardina-Salto do Boi synthetic log showing the studied stratigraphic succession, including the locations of the sampled siliciclastic sediments, the chronometric data, the grain-size and clay mineralogy results, the inferred sedimentary processes, and the respective depositional environment interpretations.

GFU 5, were drawn and their raw materials were determined; additionally, along with all the lithic materials recovered during the excavation of GFUs 6 to 8, the stone fragments were plotted in three dimensions.

Lithic raw material sources of stone tools have been determined by macroscopical comparisons with samples collected in the Côa Valley region and Western Iberia, and the characterisation of non-local flint and silcrete was complemented by a systematic binocular examination of the microfacies and examination of thin sections for selected archaeological pieces following the methodology discussed in previous publications (Mangado Llach, 2002; Aubry et al., 2012b).

The knapped lithic materials have been counted and studied using a technological approach to assess reduction sequences and to define the blank selected and retouched tool types (Demars and Laurent, 1992; Boëda, 1993; Dibble and Bar-Yosef, 1995; Pelegrin, 1995; Zilhão, 1997; Mourre, 2003). The assemblages have been analysed in terms of variations in the mass ratios of cores to blanks and blanks to tools to demonstrate, by their technological and typological attributes, the integrity of each assemblage and its technical and cultural affiliation.

Refitting of knapped and heated lithic materials used in fire structures to infer both anthropic and sedimentary processes, and to assess palimpsest formation and stratigraphic integrity (Villa, 1982; Hofman and Enloe, 1992; Deschamps and

Zilhão, 2018), has been applied systematically to the lithic materials of GFUs 8 to 4.

Age determination

The chronological data were obtained using OSL on K-rich feldspar and quartz-rich extracts from 11 sediment samples (Table 1). Cleaned quartz and K-rich feldspar grains (180–250 μm) were derived from the sediment by sieving, soaking in HCl, H_2O_2 , heavy liquid separation (2.58 g cm^{-3}), and finally etching in 40% HF (quartz) or 10% HF (feldspar) before a final wash in HCl (Aitken, 1985, 1998). Only very limited amounts of feldspar could be extracted from these samples.

All OSL signals were measured using automated Risø TL/OSL DA-20 readers (Bøtter-Jensen et al., 2010) equipped with arrays of blue (470 \pm 30 nm) and infrared (IR, 870 \pm 40 nm) LEDs providing stimulation powers at the sample position of approximately 80 and 130 mW/cm^2 , respectively. The post-IR blue quartz signals (8 mm aliquots) were detected in an ultraviolet window (Hoya U-340), whereas IR feldspar signals (2 mm aliquots) were detected in a blue-violet window (Schott BG3 and BG39).

The single-aliquot regenerative-dose (SAR) procedure (Murray and Wintle, 2000) was used for equivalent dose determination. For quartz, a double SAR procedure (Banerjee et al., 2001) employing IR stimulation (at 50°C for 40 s) prior

Table 1. Summary of OSL data for the Cardina-Salto do Boi reference section. Q is quartz and KF is K-rich feldspar extracts. w.c. is the field water content. D_e is the equivalent dose estimate, and n_x and N_x are the number of accepted and measured aliquots, respectively. D_e KF has been derived from pIRIR(50,225) measurements. The fading-corrected KF ages (Age KF_{corr}) has been derived by correction for fading (measured to be $1.30 \pm 0.15\%$ /decade, Auclair et al., 2003), and these ages are expected to be the most accurate estimates of burial ages for these samples.

Sample	Depth (cm)	w.c. (%)	Dose rate Q (Gy/ka)	D_e Q (Gy)	n_Q	N_Q	Dose rate KF (Gy/ka)	D_e KF (Gy)	n_{KF}	N_{KF}	Age Q (ka)	Age KF _{uncorr} (ka)	Age KF _{corr} (ka)
172219	270	0	4.90 ± 0.24	-	0	6	5.83 ± 0.25	417 ± 7	8	8	-	71.4 ± 3.2	80.3 ± 3.6
172206	193	4	4.96 ± 0.26	172 ± 21	4	6	5.89 ± 0.27	267 ± 4	8	8	35 ± 5	45.4 ± 2.1	51.0 ± 2.4
172207	190	4	4.37 ± 0.22	161 ± 27	3	6	5.30 ± 0.23	235 ± 7	6	6	37 ± 6	44.4 ± 2.4	49.9 ± 2.7
172208	179	4	4.91 ± 0.23	177 ± 15	5	6	5.85 ± 0.24	229 ± 6	8	8	36 ± 3	39.1 ± 1.9	43.9 ± 2.1
172209	170	4	4.65 ± 0.22	171 ± 23	6	6	5.59 ± 0.23	214 ± 3	18	18	37 ± 5	38.2 ± 1.6	42.9 ± 1.9
172210	161	2	4.82 ± 0.25	189 ± 40	5	6	5.76 ± 0.25	203 ± 2	7	8	39 ± 8	35.2 ± 1.6	39.5 ± 1.8
172211	153	3	4.80 ± 0.25	217 ± 33	6	6	5.74 ± 0.26	172 ± 7	6	6	45 ± 7	29.9 ± 1.8	33.6 ± 2.0
172212	145	3	4.85 ± 0.24	129 ± 10	5	6	5.79 ± 0.24	163 ± 5	7	8	27 ± 3	28.1 ± 1.5	31.5 ± 1.6
172213	136	2	4.64 ± 0.23	136 ± 27	6	6	5.58 ± 0.24	143 ± 5	6	6	29 ± 6	25.6 ± 1.5	28.7 ± 1.6
172214	130	1	4.75 ± 0.23	143 ± 11	6	6	5.69 ± 0.24	130 ± 5	11	11	30 ± 3	22.8 ± 1.3	25.6 ± 1.4
172215	118	2	4.91 ± 0.24	134 ± 24	6	6	5.84 ± 0.25	143 ± 11	6	6	27 ± 5	24.5 ± 2.2	27.5 ± 2.5

to blue (at 125°C for 100 s) and a test dose of 20 Gy was used on all samples to minimise the effects of any feldspar contamination. A preheat temperature of 260°C for 10 s and a cutheat temperature of 220°C was used for all dose measurements. A high-temperature blue bleach at 280°C for 40 s was inserted in between each SAR cycle to minimise potential recuperation effects (Murray and Wintle, 2003). The signal was summed over the initial 0.5 s of stimulation and the background over the subsequent 0.5 s of stimulation.

For feldspar, two post-IR IR (pIRIR) SAR protocols were used (Thomsen et al., 2008; Buylaert et al., 2009; Thiel et al., 2011). The pIRIR(50,225) protocol used a preheat (held for 60 s) at 250°C, a first IR stimulation at 50°C (200 s), a second stimulation at 225°C (200 s), and a high-temperature (280°C) IR exposure (200 s) after each SAR cycle. The pIRIR(50,290) protocol used a preheat of 320°C (60 s), a first IR stimulation at 50°C (200 s), a second stimulation at 290°C (200 s), and a high-temperature (320°C) IR exposure (200 s) after each SAR cycle. For both protocols, the test dose (TD) was chosen to approximately match the size of the natural dose (D_e) (i.e., $TD/D_e \in [0.7; 1.2]$). Calculations were based on the signal derived from the initial 2 s of the post-IR IR-stimulated luminescence (IRSL) minus a background derived from the last 50 s. Age-depth modelling was performed using Bayesian Statistics (Bacon script, Blaauw and Christen, 2011).

Dose rates were determined using high-resolution gamma spectrometry calibrated as described in Murray et al. (1987, 2018) and the conversion factors of Guérin et al. (2011). Before counting, crushed and homogenised samples were mixed with wax, cast in a fixed cup-shaped geometry, and stored for a minimum of 21 days (>5 ^{222}Rn half-lives) to ensure equilibrium between ^{222}Rn and ^{226}Ra . For K-feldspar extracts, the internal beta dose rate of ^{40}K was calculated assuming an effective K concentration of $12.5 \pm 0.5\%$ (Huntley and Baril, 1997). We also assume that the present-day burial depths represent the lifetime burial depths, and cosmic ray

contributions are based on Prescott and Hutton (1994). Lifetime water contents are based on measured (field) values.

RESULTS

Cardina-Salto do Boi site stratigraphy

The field description of the cross section exposed in areas excavated between 1997 and 2018 revealed a 5-m-thick stratigraphic succession (on a phyllite bedrock), articulated into eight field units (GFUs 1 to 8) and grouped in two main geoarchaeological complexes (GCA and GCB), as shown in Figures 4 and 5. From top to base, GFUs 1 and 2 are massive and bioturbated coarse units (slightly gravelly), with a poorly to very poorly sorted muddy sand fraction (sand 54–58%, silt 38–42%, and clay 4–5%) (see Fig. 5, Supplementary Figs. 1 and 2). GFU 3 is separated from the previous uppermost units by an irregular bounding surface (d0). Both GFU 3 and 4 are distinguished from GFUs 1 and 2 by relatively higher silt (44–50%) and clay (8–11%) contents, matched by a reduction in gravel content. The lower bounding surfaces of both GFU 3 and 4 are characterised by important anthropogenic processes (near d1 and d2), with a main erosive unconformity between GFUs 4 and 5 (d2). The rest of the GFUs (from 5 to 8) consist of tabular fine-grained bodies with recurrent grain-size characteristics such as low gravel content (3–7%, very slightly gravelly) and a very poorly sorted sand and mud fraction enriched in both silt (42–55%) and sand (33–47%), with only secondary amounts of clay (10–15%). A planar to irregular bounding surface, ranging from non-erosive to slightly erosive in nature, separates GFUs 5 and 6 (d3). Some intercalation of apparent incipient pedogenetically altered horizons can also be inferred in the middle part of GFU 5, as well as along the GFU 6 and 7 boundary. GFUs 6 to 8 also contain some lenticular layers of well-rounded coarse to very coarse gravel (see Fig. 5). The contact between

the local siliciclastic sedimentary infill and the bedrock is represented by a main erosive unconformity (d4).

Six grain-size components stand out (see Supplementary Fig. 1). In decreasing order of contribution these are as follows: (i) 41–55% medium to fine silt (24 μm to 14 μm , mean 18 μm) in GFUs 4 to 8, slightly lower in GFUs 1 to 3 (23–30%) and higher (58%) near the d1 unconformity (with anthropogenic accumulation of material, see Fig. 5); (ii) 11–33% medium to fine sand (303 μm to 206 μm , mean 241 μm) in GFUs 1 to 7 and 7–9% in GFU 8; (iii) very variable amounts (8–43%) of very fine sand (98 μm to 82 μm , mean 87 μm) in all GFUs; (iv) 2–8% coarse sand (986 μm to 574 μm , mean 843 μm) in GFUs 1 to 7, absent in GFU 8; (v) 3–8% ultrafine particles (mean 0.4 μm) around the d2 main unconformity and in the middle part of GFU 5 (samples C5d–C5g), as well as in GFUs 6 and 7; and (vi) 2–4% clay (mean 3 μm) in the upper part of GFU 5 (first levels with Upper Palaeolithic materials) and in GFU 8.

Illite is clearly dominant (73–94%) in all sampled sediments, with kaolinite at only 3–23%. However, clay mineralogy clearly differentiates the samples collected from the more superficial field units from those from the deeper units (see Fig. 5). GFUs 1 and 2 contain more illite (73–87%) than kaolinite (5–15%), small amounts of vermiculite (3%), chlorite (4–5%) and 10–14Å mixed-layer clays (1–4%). The remaining samples collected in GFUs 3 to 7 almost always contain vestiges of vermiculite (2–4%), with few 10–14Å mixed-layer clays (5–7%) in the middle position of GFU 5 (samples C5e and C5f; see Fig. 5); the only exception is the set of samples from the lowermost stratigraphic position (GFU 8) that contain moderate amounts of smectite (2–12%) in addition to the usual illite and kaolinite. The illite to kaolinite ratio only varies slightly within all sampled sediments, although the proportion of kaolinite increases stratigraphically upwards and thus tends to be higher in the relatively coarser units (see Fig. 5). In addition, kaolinite content is relatively higher (23–15%) in the samples collected immediately below the obvious unconformities (i.e., present-day surface, d0, d1, and d2; see Fig. 5), as well in the sample C5d (12%).

All samples have 10Å illite peak widths of below 0.15, indicating that illite crystallinity is extremely high. Eighty-nine percent of the sediments show a ratio of 5Å/10Å illite peak intensities <0.5 (Fe/Mg-rich illite), implying little or non-chemical weathering (except in samples C5d and C8b).

Archaeostratigraphic and technological evidence

The vertical distribution of lithic materials recovered in GFUs 1 to 8 of the H'/I'-17/19 area (see Fig. 3, section A) reveals that the highest density is found in GFU 4 (Figs. 6 and 7, Supplementary Table 1). Using lithic raw material types, refitting of lithics from the base of GFU 4 to GFU 8 (recovered during excavation of the H'/I'-17/19 area) has established several sets of lithic materials from layer 4b and in the same or different UA of GFU 5 (see Fig. 6). Few links at the interface between GFU 4 and GFU 5 have been identified, and vertical distribution of the refitting sets (see Figs. 6 and 7) is

consistent with the main grain-size components (see Fig. 5, Supplementary Fig. 1). Refit links show that the components of each refit unit scatter vertically over distances < 20 cm (see Figs. 6 and 7); this pattern is considered representative of the entire alluvial sequence (GFUs 8 to 5).

Except for broken/alterated heated stones used in fire structures in GFU 5/UA24 to UA29, we have obtained a low refit ratio for all the lithic assemblages (see Fig. 6). This could be explained by the small area excavated (6 m², cf. total site area estimated as >1,000 m²) and by discard of flakes or tools produced outside the excavated area, as suggested by a low core/blank ratio (see Supplementary Table 1).

The lithic assemblages from GFUs 8, 7, and 6 are very similar in terms of raw materials and reduction method. The lithic assemblages are composed only of well-preserved, fresh-edged pieces. Varieties of the local milky, translucent, and smoky quartz, rhyolite, and quartzite pebbles have been used (Supplementary Fig. 3). Technological study and refitting sets reveal two main different productions: (i) Rhyolitic fragments and a refitted flake could correspond to the preparation of a Levallois centripetal core (see Supplementary Fig. 3, no. 3, Supplementary Table 1). Cores are under-represented, but most of the blanks correspond to a Levallois recurrent centripetal method of flake production (Boëda, 1993). Few of the flakes have been retouched into notches, denticulates, or single side-scrapers (see Supplementary Fig. 3, no. 8, Supplementary Table 1). Two flake-cleavers were found in GFU 7 (Supplementary Fig. 3, no. 4 and 7). (ii) The second technological component comprises flakes produced by Discoid centripetal methods (Boëda, 1993; Mourre, 2003; Thiébaud, 2007). A single quartz prismatic core, from GFU 6, indicates a possible production of elongated flakes (see Supplementary Fig. 3, no. 2).

Lithic assemblages from GFU 5/UA38 to UA11 are also composed of well-preserved, non-patinated, fresh-edged lithic materials. However, both faces of most pieces present concretions, with magnesium (Mg) on the upper face and silicon (Si) on the lower. Varieties of the local milky, translucent quartz, rhyolite, quartzite pebbles, and regional rock crystal have been used (see Fig. 7). The lithic assemblage reveals two different methods of reduction. The most frequent corresponds to pseudo-Levallois triangular and centripetal flakes produced by Discoid centripetal unifacial to polyhedral methods (Fig. 8). A few blanks were retouched into single, double, or convergent side-scrapers, notches, and denticulates (see Fig. 8, Supplementary Table 1). The second component, found in fine-grained milky quartz between GFU 5/UA29 to UA24 and in rock crystal in GFU 5/UA16–18, corresponds to the production of small quadrangular flakes and possibly bladelets on prismatic cores (Supplementary Fig. 4). One flake produced by this reduction method has been truncated (see Supplementary Fig. 4, no. 5).

Lithic materials from GFU 5/UA10 to GFU 5/UA1 show a radical change, in both technology and raw material. This assemblage was made from regional and local quartz, quartzite, and rock crystal, as well as flint and silcrete from distant sources in central Iberia (northern Meseta) and central

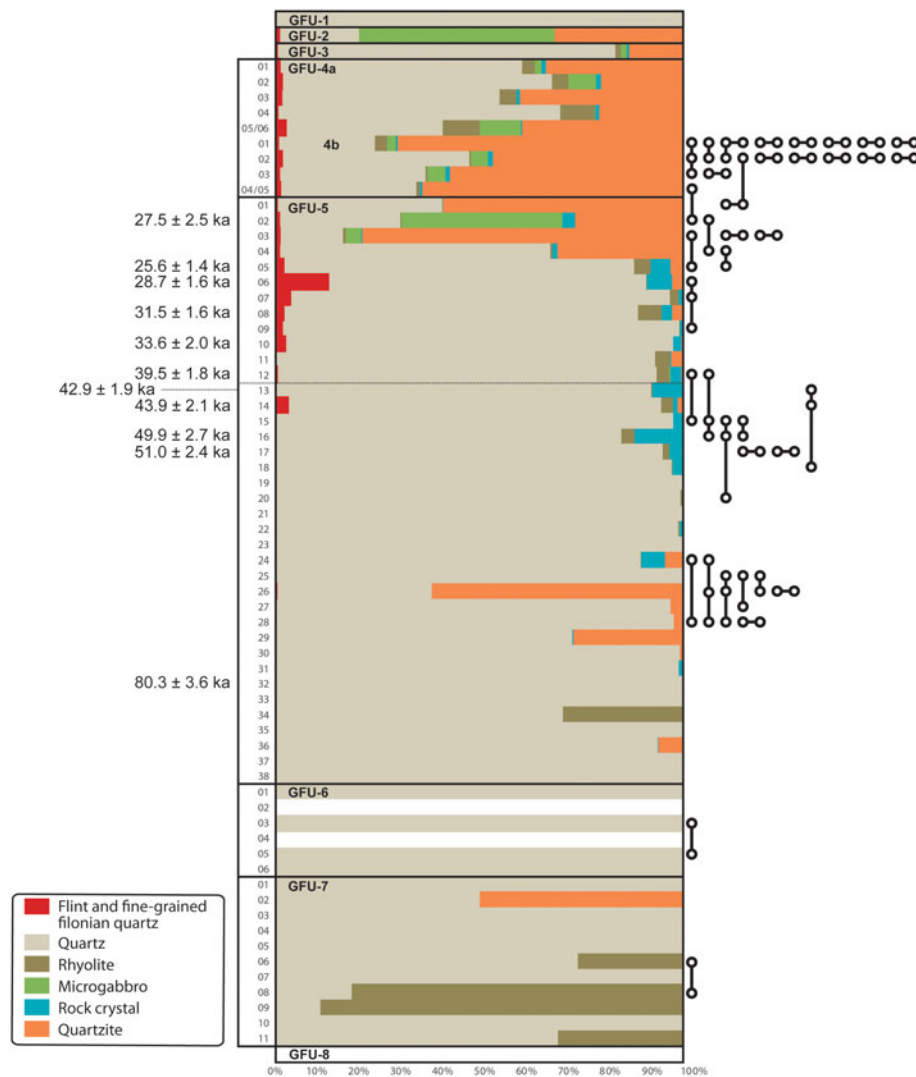


Figure 6. (color online) Stratigraphical position of the radiometric luminescence data, artificial units by geoarchaeological field unit (GFU), raw material proportions of knapped lithic materials, and vertical distribution of the refitting sets.

Portugal, which are found throughout the Upper Palaeolithic in the Côa Valley (see Fig. 6; Aubry et al., 2012b). GFU 5/UA10 to UA2 contain blades produced on prismatic unipolar cores and prepared by a central cresting (Fig. 9, no. 19, 20, and 21) and bladelets produced on carinated or burin-type cores (see Fig. 9, no. 1, 2, 6, 7, 8, 15, 16, and 17). This lithic assemblage set is defined by the use of a specific regional filonian brown jasper (see Figs. 8 and 9, no. 15–21), absent in all the other stratigraphic units (although a single blade fragment, probably intrusive, has been recovered in the GFU 5/UA14, see Fig. 9, no. 20) and confirmed by the vertical distribution of the refitting set (see Fig. 7). None of the fragmented jasper blades was transformed into a tool. However, some bladelets of this raw material exhibit the technological characteristics of burin and carinated nose-scraper core reduction strategy on blade fragments, the latter being absent from the assemblage (see Fig. 9, no. 15–17). Some flint and silcrete bladelets were transformed into Dufour bladelets of the subtype Dufour (see Fig. 9, no. 13), Font-Yves bladelets (see Fig. 9, no. 12; Demars and Laurent, 1992), and a Caminade

endscraper (see Fig. 9, no. 14; Sonnevile-Bordes and Mortureux, 1956).

The first 20 cm of GFU 5 (UA1 to UA4) yielded retouched bladelets, micro-gravette point fragments (Supplementary Fig. 5, no. 27), and several Noailles burins (Demars and Laurent, 1992) made from long-distant flint and silcrete sources and from regional rock crystal (see Fig. 6, Supplementary Fig. 5, no. 28, 29, 31).

Layer 4b is represented by a large circular-shaped structure of stone fragments, mostly heated (see Fig. 4), and associated with a lithic assemblage of micro-gravette points and retouched bladelet fragments (Supplementary Fig. 5, no. 1–26). Flint and silcrete long-distance sources are also represented (Aubry et al., 2012b). Bladelet reduction comprises prismatic, burin core, and bipolar strategies.

Luminescence dating

The 11 sediment samples dated by luminescence (172206 to 172215 and 172219, see Table 1) were collected in metal

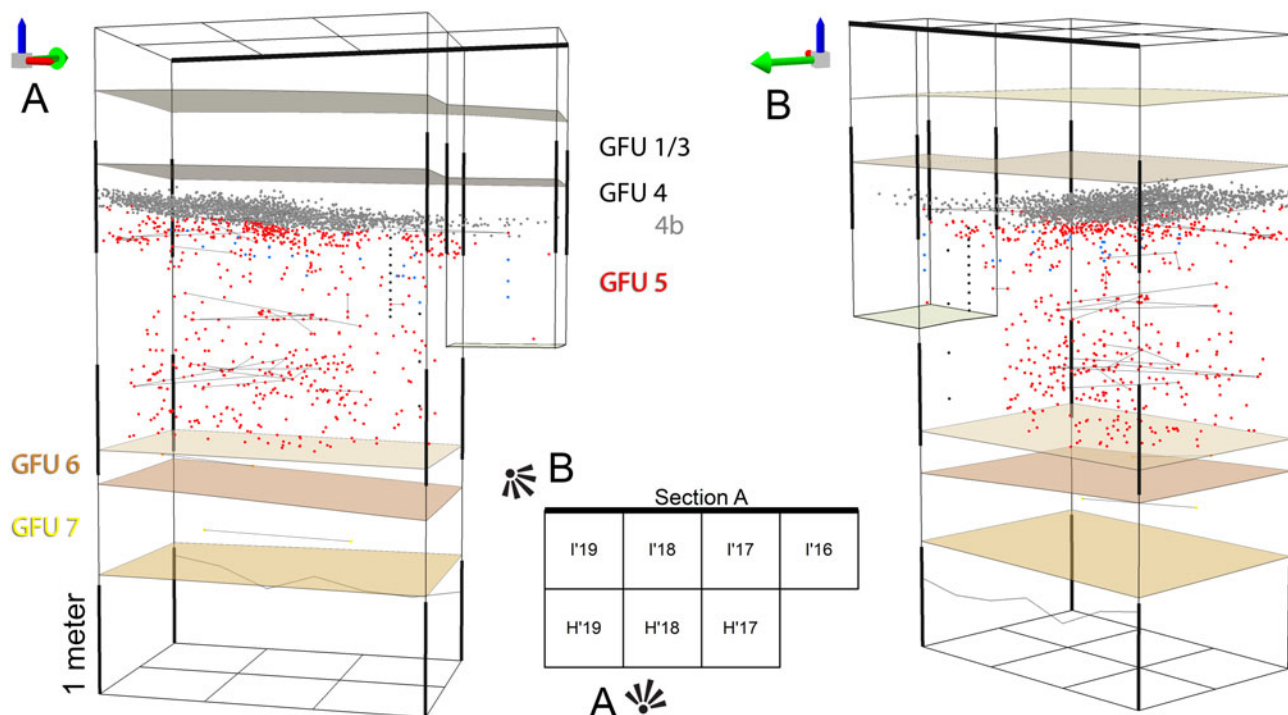


Figure 7. Three-dimensional plot of all lithic materials over 5 cm in geoarchaeological field unit (GFU) 4b (grey dots) and GFU 5 (red dots) and refitting links of knapped and heated-fracture lithic materials (lines). In GFU 6 (orange dots) and GFU 7 (yellow dots), only refitted material is presented. Jasper lithics in GFU 5 are represented in blue, and dating samples are in black. (For interpretation of the references to color in this figure legend, the reader is referred to the web version of this article.)

tubes from cross-section A of the H'/I'-17/19 test area (see Fig. 3) in GFU 5 under a large circular stone structure defining layer 4b (see Fig. 4). GFUs 6, 7, and 8 were not sampled because they were not exposed until excavation in 2018, after sampling in April 2017.

Initial quartz measurements showed that the OSL signals were not fast-component dominated, and that a significant number (ranging between ~15% and 100%) of sensitivity-corrected natural OSL signals (L_n/T_n) appeared to be in saturation on the laboratory dose response curve. When fitting the dose response curves with a saturating exponential function (of the form $L_x/T_x = a[1 - \exp(-x/D_0)]$, where x is the laboratory dose, and a and D_0 are constants), the average D_0 value is 65 ± 2 Gy. Except for the youngest four samples (i.e., 172212-15) all quartz dose estimates are considerably above $2 \times D_0$ and thus not likely to be accurate estimates of the burial dose; this is particularly true for samples 172206-11 and -19.

On the other hand, the signals from the K-rich feldspar extracts are well behaved with an average D_0 value of 392 ± 6 Gy ($n = 91$, pIRIR(50,225)). All feldspar dose estimates are well below $2 \times D_0$ and thus likely to be accurate estimates of the burial dose (at least from the perspective of dose estimation). A pIRIR(50,225) dose recovery experiment on sample 172209, where the aliquots were first bleached for 2 h in a solar simulator and subsequently given a beta dose of 300 Gy, gave a satisfactory dose recovery ratio of 0.96 ± 0.03 ($n = 6$, using a TD of 300 Gy). A similar experiment using the pIRIR(50,290) protocol gave an unsatisfactory dose recovery

ratio of 0.78 ± 0.02 ($n = 6$). Thus, based on the dose recovery results, the pIRIR(50,225) protocol is more likely to give accurate dose estimates. Nonetheless, it is informative to investigate the dose correlations between the doses measured for the different feldspar signals, bearing in mind the order of the signals $IR(50) > pIRIR(50,225) > pIRIR(50,290)$, in terms of both anomalous fading and bleachability (e.g., Buylaert et al., 2012). In Figure 10a, the equivalent doses measured for IR(50) and pIRIR(50,290) are plotted against those from pIRIR(50,225), together with the linear regressions of the data, $y = 0.77x - 0.7$ Gy and $y = 1.11x + 32$ Gy, where x is the pIRIR(50,225) dose and y is the IR(50) and pIRIR(50,290) dose, respectively. It is expected that the IR(50) doses will fall below the 1:1 line and the pIRIR(50,290) doses above due to anomalous fading of both the IR(50) and pIRIR(50,225) signals. The intercept of the IR(50) fit is consistent with zero, showing that the pIRIR(50,225) signal is likely to be well bleached (Murray et al., 2012). The pIRIR(50,290) data has an intercept of ~30 Gy, implying that this signal has a small residual dose arising because this signal is more difficult to bleach than the other two, and because of this these ages are not considered further.

Standard fading-rate measurements (Auclair et al., 2003) gave a g -value of $3.29 \pm 0.15\%$ /decade and $1.30 \pm 0.16\%$ /decade normalised to 2 days ($n = 6$) for IR(50) and pIRIR(50,225), respectively. Fading correction using these g -values increases the age estimates by ~36% and ~12%, respectively. The average ratio of the fading-corrected IR(50) to pIRIR(50,225) ages is 0.92 ± 0.01 ($n = 11$). Given the smaller



Figure 8. (color online) Lithic industries from ge archaeological field unit/artificial unit GFU 5/UA38 to UA10 and stratigraphical position.

fading correction for the pIRIR(50,225) signal, we regard these ages as the most reliable.

A synthesis of luminescence data obtained for GFU 5 is presented in Table 1. For the younger ages the quartz and the corrected pIRIR(50,225) ages are consistent with each other; for older ages quartz tends to underestimate, presumably because of saturation effects in quartz. Although the larger quartz uncertainties limit the value of this comparison, this agreement also suggests the pIRIR(50,225) signals were sufficiently bleached at the time of deposition, which is also supported by the proportional relationship between IR(50) and pIRIR(50,225) doses in Figure 10a.

Figure 10b shows the fading-corrected pIRIR(50,225) ages as a function of depth. Bayesian age-depth modelling was performed using the Bacon code (Blaauw and Christen, 2001). The stratigraphic boundary between the Middle and Upper Palaeolithic lithic technology was discussed above as lying between 153 cm and 161 cm (see Figs. 4 and 6). Age-depth modelling quantitatively constrains the timing of this

Middle-to-Upper Palaeolithic transition to between 34.0 ± 1.4 ka (153 cm) and 38.4 ± 1.1 ka (161 cm, see Fig. 10b; random uncertainties only). As is standard in luminescence dating, the uncertainties in the ages are given at the 68% confidence interval. The uncertainties derived from Bayesian modelling only include the random component; typical systematic uncertainties are $\sim 4\%$, and so the age of the Middle-to-Upper Palaeolithic boundary (including all known sources of uncertainty) lies between 34.0 ± 2.0 ka and 38.4 ± 1.9 ka.

DISCUSSION

Sedimentary processes and depositional environments

Facies analysis, coupled with grain-size and clay mineralogy results, allows the interpretation of sedimentary processes and

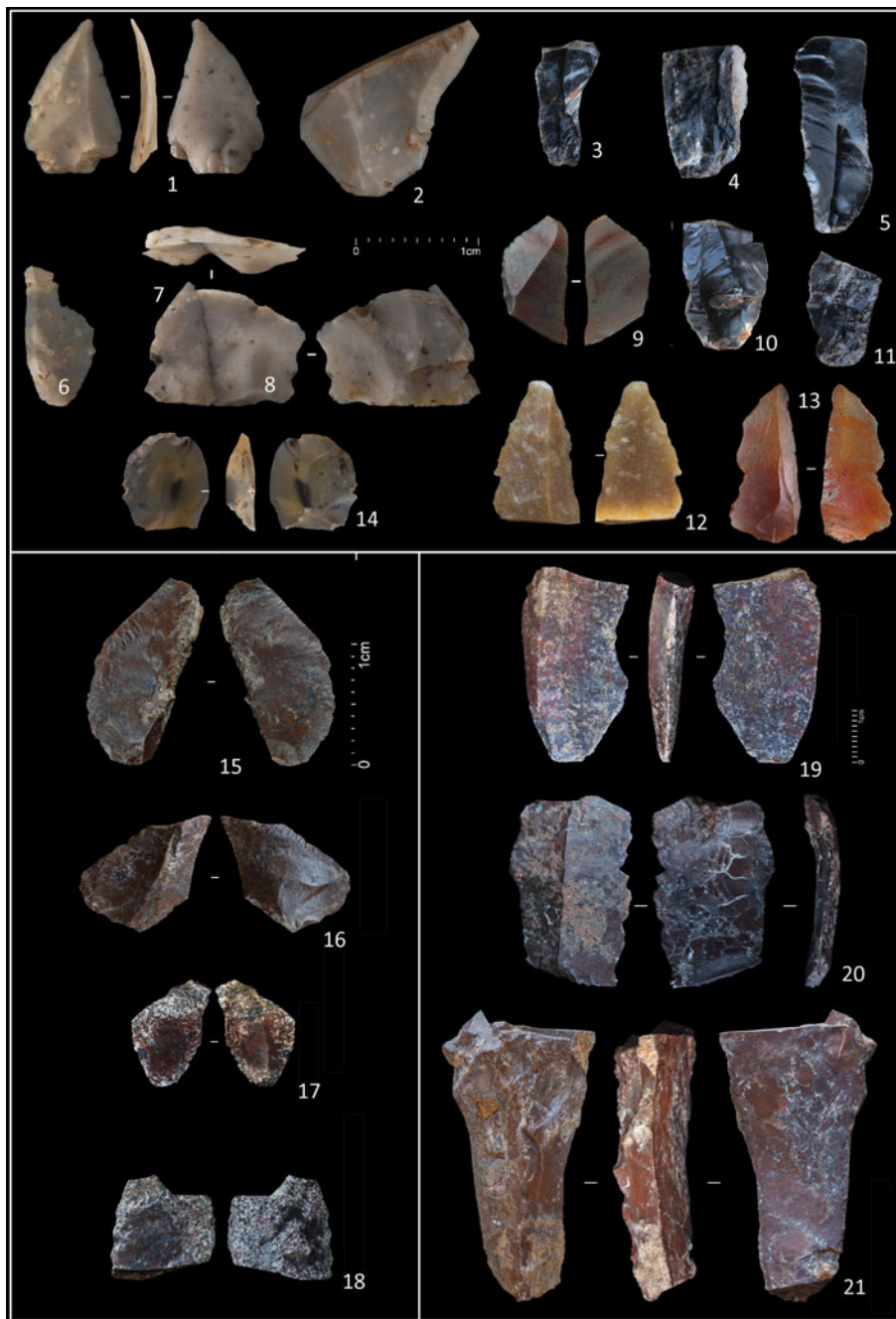


Figure 9. (color online) Lithic industries from geoarchaeological field unit/artificial unit GFU 5/UA14 (no. 20), UA10 (no. 19), UA8 (no. 3), UA7 (no. 18), UA6 (no. 1, 12, 17, and 21), UA5 (no. 7, 14, 15, and 16), UA4 (no. 4, 5, 6, 9, 10, and 11), UA3 (no. 8 and 13), and UA2 (no. 2). Bladelets produced on carinated or burin-type cores (no. 1, 2, 6, 7, 8, 15, 16, and 17), retouched bladelets (no. 3, 4, 5, 9, 10, 11, and 18), Dufour bladelets of the subtype Dufour (no. 13), Font-Yves bladelets (no. 12), Caminade endscraper (no. 14.), and blade fragments (no. 19, 20, and 21).

provides a better understanding of changes in the depositional environment of the Cardina-Salto do Boi stratigraphic succession; they can also explain some dating results.

The presence of several modes in clastic sediments from hydraulic continental environments can reflect either multiple sedimentary sources or different transport mechanisms (Sun et al., 2002; Liu et al., 2018; among others). This understanding helps in the interpretation of the results of grain-size

polymodal decomposition. The first (i), third (iii), and last (vi) grain-size components, consisting of medium to fine silt, very fine sand, and clay, respectively, represent accumulation from suspension load after fluvial sediment input. This, of course, depends on the available source material and water energy (Torres et al., 2005; Xiao et al., 2015). In contrast, the coarse particles (from $\sim 200 \mu\text{m}$ to $1000 \mu\text{m}$) from the second (ii) and fourth (iv) grain-size components would indicate

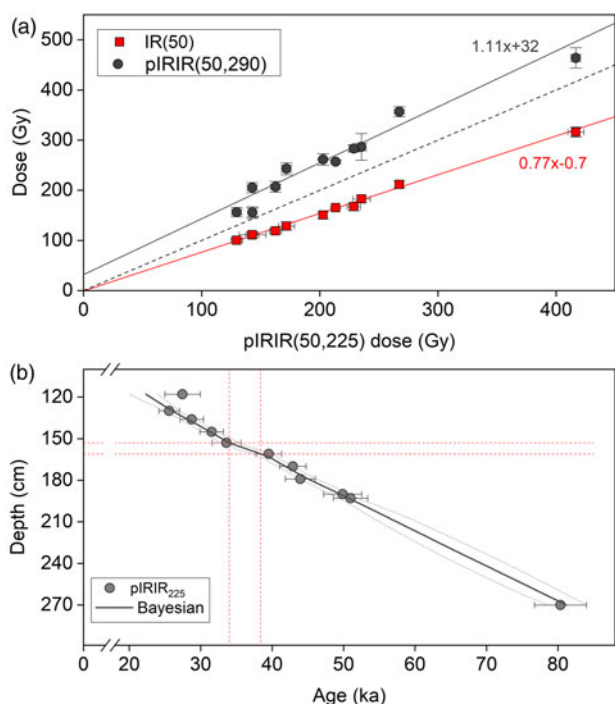


Figure 10. (a) K-feldspar doses: IR(50) (squares) and pIRIR (50,290) (circles) as a function of pIRIR(50,225) doses. Also shown are the linear fits to the data. (b) Fading-corrected pIRIR (50,225) ages. A g -value of $1.30 \pm 0.16\%/decade$ ($n = 6$) was used to correct for fading. The uncertainty ranges of 68% are shown for these ages. Also shown is age-depth modelling using Bayesian Statistics (Bacon script; Blaauw and Christen, 2001). The dotted lines represent the 68% confidence interval. Also shown (red dashed lines) is the transition from the Middle to the Upper Palaeolithic occurring in the depth range between 153 cm (34.4 ± 1.4 ka) and 161 cm (38.4 ± 1.1 ka). (For interpretation of the references to color in this figure legend, the reader is referred to the web version of this article.)

transport by traction current from proximal sources (Sun et al., 2002). In addition, the ultrafine particles from the fifth (v) grain-size component ($<1 \mu\text{m}$) can be related to chemical weathering and pedogenesis (e.g., Paton, 1978; Bronger and Heinkele, 1990).

The illite-dominated clay fraction is mainly of very high crystallinity and is Fe/Mg-rich; this indicates relatively unaltered clay mineralogy, largely determined by the geology of the sourced areas (Keller, 1970; Chamley, 1989). Here, this can be explained by the proximity to rapidly eroding mica-rich Precambrian–Palaeozoic metasedimentary rocks.

The observed slight increase in the kaolinite/illite ratio with position upwards in the studied stratigraphic succession may suggest an evolution with time towards relatively more humid conditions but still within a generally cold context. The presence of smectite (limited to the lower part of the succession) is also compatible with a climate with contrasting seasons (Singer, 1980, 1984; Chamley, 1989) during the deposition of GFUs 7 and 8.

In addition, the presence of some post-depositional overprinting of the clay minerals must be considered. This

includes: (i) enrichment of vermiculite and the 10–14 Å mixed-layer clays close to the present-day land surface (GFUs 1 and 2) and in the upper levels containing the last Middle Palaeolithic material (in GFU 5), presumably due to the deterioration of mica-type minerals under low pH conditions, (e.g., by pedogenetic processes) (Singer, 1980; Chamley, 1989; Braga et al., 2002; Pe-Piper et al., 2005); (ii) alteration of muscovite/biotite and/or feldspar to chlorite in GFUs 1 and 2, also linked to pedogenesis; (iii) meteoric water infiltration and flushing, during sub-aerial exposure of the sediments, with kaolinite increasing near erosive unconformities (with anthropogenic inputs and disturbances), as well as just below an inferred non-depositional unconformity (a hiatus with no evident erosion in GFU 5) at the archaeologically attested Middle–Upper Palaeolithic transition (see Figs. 5 and 6). This is confirmed by the relatively higher content of the ultrafine grain-size fraction (see Supplementary Fig. 1).

In summary, in terms of formation processes at the site, the Cardina-Salto do Boi sedimentary infill started with accumulation in a fluvial environment, between 5 m and 3.5 m below the present-day surface (GFUs 8 to 6), under low-energy diffusive water-flow conditions with the settling of suspended fine sediments dominant over bedload deposition (overbank sedimentation). This occurred relatively closer to the palaeo-channel, where the decrease in water-flow energy (dominated by low-water vertical accretion) was most rapid. In the 3.5 m to 1 m interval (GFU 5) vertical sedimentary accretion continues, now relatively more distant from the paleo-fluvial channel; this deposition is interrupted by environmental stabilisation phases with no evident erosion. A new phase of overbank sedimentation then took place before an important erosive phase (d2) and anthropogenic accumulation of material (see Fig. 5). The uppermost ~ 1 m of sedimentary thickness (GFUs 1 to 4) reflects slope deposition, under the control of gravity-driven processes, accumulating with the concurrent action of water (though with some evidence of pedogenesis) and anthropogenic inputs/disturbances and redepositions.

Thus, the two local geoarchaeological complexes identified here are interpreted in terms of depositional environment as follows (from bottom to top): (i) GCB = a relatively stable floodplain sequence with some nuisance flooding caused either by overbank floods or by rising groundwater levels and linked to generally continuous and low-intensity meteoric precipitation initially under a more temperate and humid climate (with some seasonality) that evolved to colder conditions; GCA = a subsequent period of progressive increase in humid conditions and chemical weathering attested by the more superficial disturbed slope sequence (colluvium), driven by gravity processes and shallow surface water flow.

Links between refitted lithic materials show a vertical distribution pattern over distances <20 cm in GFUs 5 to 7 (see Fig. 6) that should result from reworking related to the rapid decrease in water-flow energy at the end of the alluvial floodplain process of sedimentation. The three-dimensional distribution and orientation of refitted pieces indicate that

lithic materials were affected by low-magnitude post-depositional non-anthropogenic alluvial displacement in conformity with accumulation in a fluvial environment under low-energy, diffuse water-flow conditions (see Fig. 7).

Cultural attribution of lithic assemblages

Technological study of Middle Palaeolithic lithic assemblages of Portugal and the Iberian inland is incipient, and well-dated archaeostratigraphic sequences giving information on the techno-cultural evolution patterns of Neanderthal technology are sparse (Raposo, 1995; Zilhão, 2001; Cardoso, 2006; Zilhão et al., 2011). The Gruta da Oliveira (see Fig. 1) archaeostratigraphical succession, dated by U/Th, has been studied using a taphonomical/technical approach. The study shows a shift, during late marine oxygen isotope stage (MIS) 5 or early MIS 4, from the centripetal Levallois reduction, associated with rare bifaces and flake-cleavers to Discoid and Kombewa debitage (Deschamps and Zilhão, 2018). Despite the small area excavated, the lithic assemblages of GFUs 8 to 6 at the Cardina-Salto do Boi site have characteristics in common with layers 15 to 27 of the Gruta da Oliveira archaeostratigraphy.

Discoid reduction methods found throughout GFU 5/UA38 to UA11 are widespread in Iberian Middle Palaeolithic assemblages dated to MIS 5 and MIS 4 (Deschamps and Zilhão, 2018). Despite some variation along the GFU 5 stratigraphy of Cardina-Salto do Boi, and possible production of small flakes and bladelets, the selection of local raw materials and the technology used to produce flakes are similar, with no indication of the bidirectional blade reduction sequence or bifacial technology that characterise the Middle-to-Upper Palaeolithic transitional lithic assemblages.

The GFU 5/UA10 to UA1 lithic assemblages are distinct and can be assigned by their typology and technology to the Upper Palaeolithic. Different lithic assemblages can be defined based on raw materials, reduction strategies, and tool types. The lithic assemblage recovered from GFU 5/UA10, defined by the use of brown jasper (see Fig. 8), comprises blade debitage, several examples of the Roc-de-Combe subtype Dufour and Font-Yves bladelets, and a Caminade endscraper. These are typical index fossils of the Evolved Aurignacian (Rigaud, 1982; Demars and Laurent, 1992; Morala et al., 2005; Michel 2010). In Portugal, the lithic assemblages from a cluster of open-air sites in the Rio Maior basin and the Lower Mondego valley, and caves in the Alentejo and Estremadura regions, exhibit blade debitage on prismatic unipolar cores prepared by cresting and bladelets produced on carinated or burin cores. These assemblages have previously been assigned to the Final or Evolved Aurignacian (Zilhão, 1997, 2006b; Aubry et al., 2006). The end of the Aurignacian in southern France has been dated by radiocarbon to approximately 32,000 cal yr BP (Michel, 2010; Higham et al., 2011; Rigaud et al., 2016), and the Brignol (Lot-et-Garonne, France) open-air occupation, yielding Caminade endscrapers and Roc-de-Combe Dufour bladelets, has been dated by OSL to 33–34 ka (Anderson et al., 2016).

The Noailles burins from the top of GFU 5 are a diagnostic stone-tool type only known in the Early and Middle Gravettian contexts of France, northern Spain, and Italy. Gravettian occupations with Noailles burins have provided ^{14}C ages covering a wide period between 28,000 and 32,000 cal yr BP (Klaric, 2015; Peña Alonso, 2010; Foucher et al., 2011; Rigaud et al., 2016).

New data for the timing of the Middle-to-Upper Palaeolithic transition in Iberia

Different models have been proposed for the timing and nature of the Middle-to-Upper Palaeolithic transition in Iberia, based on radiometric dating of archaeological layers and lithic assemblage technology. The reevaluation of the stratigraphical contexts and the application of new dating procedures have led some authors to consider that Neanderthal populations did not survive much longer in the Iberian Peninsula than in the rest of Europe (Maroto et al., 2012; Wood et al., 2013; Higham, et al., 2014; Alcaraz-Castaño et al., 2017). Based on luminescence dating of loess deposits from the Upper Tagus Basin, it has been suggested that the abandonment of the interior of Iberia by Neanderthals occurred 42 ka ago, and that, as a direct consequence of a pronounced environmental aridity, inner territories were uninhabited until 28 or 25.5 ka. In this model, any persistence of Neanderthals until 37 ka was restricted to coastal areas (Wolf et al., 2018). Others have accepted a late survival of Neanderthals in Iberia and proposed possible isolation and survival of residual Neanderthal groups more recently than 30 ka in ecological refuge zones in marginal mountain areas of the Cantabrian region (Baena et al., 2018) or in the south-western Iberian Peninsula (Finlayson et al., 2006; Jennings et al., 2011).

After the recent revisions of Middle-to-Upper Palaeolithic sites, improvements in pre-treatment used for samples dated by ^{14}C or by other dating methods, and the discovery of new sites, few Middle Palaeolithic occupation sites have provided unquestionable ages younger than 40 ka and little reliable evidence for such young existence of Aurignacian lithic technology in southern Iberia.

At the Cova de les Cendres site near Alicante (see Fig. 1), level XVI, corresponding to the lower part of the Early Upper Palaeolithic sequence, has been assigned to the Evolved Aurignacian (Villaverde et al., 2019) based on the lithic assemblage and a radiocarbon date of 35,379–34,614 cal yr BP ($31,080 \pm 170$ cal yr BP [Beta-458,3469], 2σ) using the IntCal13 calibration curve (Reimer et al., 2013).

Archaeostratigraphy, radiocarbon, and luminescence dating at Cueva Antón, located in the Mula basin of Murcia (see Fig. 1, southeastern Spain; Zilhão et al., 2016), have shown that the Mousterian layer I-k cannot be older than 37,100 cal yr BP, and at the nearby rockshelter at La Boja, the basal Aurignacian cannot be younger than 36,500 cal yr BP (Zilhão et al., 2017).

In Portugal, one bovid and two horse tooth enamel samples have been used to date the Middle Palaeolithic occupation at

the open-air site of Foz do Enxarrique to 33.6 ± 0.5 ka by U-series (see Fig. 1; Raposo, 1995), and the alluvial deposit containing the faunal remains and lithic assemblage provided an age of 38.5 ± 1.6 ka using fading-corrected IRSL (Cunha et al., 2008). However, using the pIRIR dating protocol applied at Cardina-Salto do Boi, the same archaeological level provided dates of 44 ± 3 ka, 43 ± 4 ka, and 37 ± 2 ka. The U-series and conventional IRSL ages are now considered to be underestimates when compared to pIRIR ages (Cunha et al., 2019) and do not provide reliable evidence of Neanderthal persistence after 40 ka.

The existence of Aurignacian occupation in southwestern Iberia has been debated (Zilhão, 1997; Straus et al., 2000; Zilhão and Trinkaus, 2002; Trinkaus et al., 2007; Zilhão et al., 2010; Peña Alonso and Vega Toscano, 2013; Bicho et al., 2017). Recently, the Bj-13-12 layer lithic assemblage of the Bajondillo Cave (see Fig. 1) has been attributed to the Early Aurignacian or Proto-Aurignacian based on the presence of blades and bladelet cores and the 43–41 cal yr BP dates (Cortés-Sánchez et al., 2019). However, the lead author has previously considered the same assemblage as minimal and impracticable for a reliable techno-typological analysis (Cortés-Sánchez, 2007, p. 141–142), and it cannot be clearly attributed to the Proto-Aurignacian or Early Aurignacian; rather than assign it to a chrono-cultural phase it would be wiser to consider it a mixed assemblage (Anderson et al., 2019; Peña Alonso, 2019). Nevertheless, at Cardina-Salto do Boi, lithic assemblages, stratigraphy, and dating indicate that reduction strategies other than Discoid or Levallois flake production are already present from 80 to 50 ka cal BP, attesting to reduction-scheme diversity at early stages (see Supplementary Fig. 4).

Several hypotheses based on ecological factors have been put forward to explain the apparent late survival of Neanderthal populations in the southern and western regions of the Iberian Peninsula (D'Errico and Sanchez Goñi, 2003; Finlayson et al., 2004, 2006; Zilhão, 2006a; Jiménez-Espejo et al., 2013; Zilhão et al., 2017; Carrión et al., 2019). The first of these hypotheses suggests that AMH populations bearing an Aurignacian technology may not have expanded south of the Ebro River during Interstadial 9, which occurred just prior to Heinrich Event 4 (H4, 39 ka). Based on the ages obtained in the Mula region, the spread of the Evolved Aurignacian into southern and western Iberia and the replacement of Iberian late-persisting Mousterian (~ 36.5 – 37.1 ka) has been interpreted as a response to the global climatic transition from Greenland Interstadial 8 to Greenland Stadial 8 (Rasmussen et al., 2014; Zilhão et al., 2017). This lack of expansion to the south may have been because these regions were significantly more wooded and thus less favourable, since the large mammals on which their subsistence systems were focused preferred open landscapes (Sepulchre et al., 2007).

The Greenland Interstadial 8, which followed Heinrich Stadial (HS) 4, lasted from ~ 38.2 to ~ 36.6 ka (Wolff et al., 2010). This period is associated with a strongly expressed vegetation gradient that developed at $\sim 40^\circ$ N, with temperate (deciduous oaks) and warm-temperate (Mediterranean taxa)

elements undergoing a very significant expansion to the south (Fletcher et al., 2010). The persistence of the frontier effect over several millennia has been explained by extreme aridity in the northern slopes of the Iberian Range during HS 4 and temperate forest expansion in its southern slopes during the interstadials that bracket it (Daura et al., 2012).

The new data obtained at Cardina-Salto do Boi in north-eastern Portugal, at the eastern limit of the northern Meseta, show clearly that the absence of evidence cannot be interpreted as evidence of absence. The defined lithic assemblages, refitting links (see Fig. 6), and sedimentological data (see Fig. 5) indicate that the transition between Discoid reduction-method technology and blade and bladelet production using non-local flint and silcrete sources can be placed between GFU 5/UA12 and GFU 5/UA10. The blade fragment in fine-grained jasper found in GFU 5/UA 14 (see Fig. 9, no. 20) is a unique piece made of non-local material recovered below GFU 5/UA 12 (see Fig. 6).

The ages obtained for samples 17208 (43.9 ± 2.1) and 17209 (42.9 ± 1.9) confirm the persistence of a Middle Palaeolithic Discoid reduction strategy during the temporal range of the Châtelperronian technocomplex attested in France and northern Spain (Higham et al., 2014; Marín-Arroyo et al., 2018). Considering that AMH associated with Early Aurignacian technology were established in northern Iberia from around 42,000 cal yr BP (Wood et al., 2014), the age obtained for sample 17210 and the lithic assemblage raw material types and reduction strategies support the coexistence model and indicate that Neanderthals and AMH overlapped in geographical areas in the north and west of the Iberian Plateau (see Fig. 1).

The boundary between the Middle and Upper Palaeolithic has been identified as lying between 153 cm and 161 cm (see Figs. 4 and 6). From the age-depth modelling of the luminescence dates, the age of the Middle-to-Upper Palaeolithic boundary lies between 34.0 ± 2.0 ka and 38.4 ± 1.9 ka.

Moreover, the reconstruction of the sedimentary processes and related palaeoenvironmental conditions show that, like in cave and rockshelter Iberian sites (Aubry et al., 2011; Mallol et al., 2012), the Middle-to-Upper Palaeolithic technological transition occurred during a stratigraphic disconformity (see Fig. 5, Supplementary Figs. 1 and 2), preventing a precise characterisation of the Neanderthal or AMH occupations that could have occurred during this hiatus and hampering evaluations of the continuity or discontinuity of human occupation.

The Upper Palaeolithic technology, constrained by the distribution of 28 pieces of regional filonian fine-grained jasper (see Figs. 7 and 9) that compose a lithic assemblage featuring diagnostic Evolved Aurignacian blade and carinated core-reduction strategies and stone tools (see Fig. 9); the assemblage dates to 33.6 ± 2 ka (172211, GFU 5/UA10). Attribution of the lithic assemblage to the Aurignacian is supported by the Bayesian radiocarbon age model obtained for the end of the Aurignacian in the Cantabrian region (Marín-Arroyo et al., 2018) and for the Abri Pataud sequence in southern France (Higham et al., 2011).

The age obtained for sample 172212 (31.5 ± 1.6 ka) could be related to the Middle Gravettian occupation associated with the Noailles burins from the top of GFU 5 and is in agreement with radiocarbon ages obtained for other Middle Gravettian contexts (Klaric, 2015; Peña Alonso, 2010). The ages from samples 172213 to 172215 (28.7 ± 1.6 , 25.6 ± 1.4 , and 27.5 ± 2.5 , see Fig. 10, Table 1), are statistically indistinguishable from the results obtained by TL for the base of GFU 4 (27.8 ± 1.5 , 28 ± 2.1 , 27 ± 1.8 , 26.5 ± 1.8 , and 30.1 ± 1.5 ka) in the area excavated between 1995 and 2001 (see Fig. 3; Valladas et al., 2001). The ages indicate an Upper or Late Gravettian chronology, probably related to a pit detected all around the excavated portion of the large circular stone structure (and corresponding to layer 4b, see Fig. 4).

CONCLUSION

The results obtained at Cardina-Salto do Boi since 1995 show that, in contrast to the largely accepted model for the Upper Pleistocene settlement of Iberia, the Côa Valley and the eastern limit of northern Meseta were occupied throughout the Middle and Upper Palaeolithic.

The Cardina-Salto do Boi archaeostratigraphy and OSL dating indicate that a Neanderthal-associated Middle Palaeolithic culture lived in the Côa Valley through the MIS 4 and 3. The OSL ages obtained for samples 17208 and 17209 (43.9 ± 2.1 , 42.9 ± 1.9 ka) confirm the persistence of Middle Palaeolithic technology in central Iberia during the development of “transitional” industries in northern Spain, France, and Italy. The lithic assemblage and the luminescence age obtained for sample 172210 (39.5 ± 1.8 ka) provide new evidence of the persistence of Neanderthal-associated Middle Palaeolithic material culture in some regions of Iberia after they were replaced by AMH in the rest of Europe.

Correlatively, the Late Aurignacian affinities of the lithic assemblage recovered under GFU 5/UA10 and the OSL age obtained for sample 172211 (33.6 ± 2 ka) provide new evidence contradicting the hypothesis that AMH dispersal in southern and central Iberia only occurred during the Gravettian.

Interpretation of the evolution of the depositional environment and luminescence ages reveal that the Middle-to-Upper stone-tool technology change coincides with a minor non-depositional unconformity (hiatus, with no evident erosion). Further work is needed to establish whether this disconformity of several millennia could be related to the drastic change in climatic conditions seen in the Atlantic marine record and to characterise and establish the precise chronology of human occupation during the sedimentary hiatus.

Even 25 years after the identification of the significance of the Côa Valley it is still necessary to emphasise that the Iberian inland was not a human void during the Middle and Upper Palaeolithic, and that the several colonisations, either earlier or later, were not confined to the coastline. Cardina-Salto do Boi proves that it is possible to find, in the Iberian inland, a well-preserved and significant open-air sequence

of datable deposits recording the Middle-to-Upper Palaeolithic transition.

Our results confirm that additional dating methods and the development of surveys focusing on different geomorphological settings can be used to overcome the current evidential limitations of the cave and rockshelter record and to establish more consistent models for the timing of Neanderthal disappearance and AMH expansion in the different regions of the Iberian Peninsula.

ACKNOWLEDGMENTS

This study is a contribution to the Project PALÆCOA: Neanderthal to Anatomically Modern Human transition in the Côa Valley: Environments, Symbolism and Social networks (PTDC/EPH-ARQ/0326/2014), funded by the Fundação para a Ciência e Tecnologia (FCT) and the Europe 2020 Programme—FEDER (POCI-01-0145-FEDER-016605). The Direção-Geral do Património Cultural provided the permit for this project. We thank the Fundação Côa Parque for its logistical support and permission to conduct the project on which this study is based. We also acknowledge the contribution from the Vila Nova de Foz Côa and Santa Comba Municipalities for providing logistical help for the excavation works at Cardina site.

AUTHOR CONTRIBUTIONS

A.T. and D.L. conceived the research; A.T. designed the research; A.T., B.A.F., L.L., S.A.T., S.M. performed the archaeological fieldwork; A.T., L.L. and S.A.T. performed and interpreted archaeological data; D.L. performed the facies analysis and interpreted all the sedimentological field/laboratory data (including grain-size, and XRD data with the technical help of Mr. Carlos Maia); K.T., E.R., M.A. and A.S.M. conducted the OSL analysis. A.T. and D.L. wrote the paper; and all the authors reviewed and edited the manuscript. Furthermore, all the authors have read and approved the manuscript, declaring no conflict of interest.

SUPPLEMENTARY MATERIAL

The supplementary material for this article can be found at <https://doi.org/10.1017/qua.2020.43>.

REFERENCES

- Aitken, M.J., 1985. *Thermoluminescence Dating*. Academic Press, London.
- Aitken, M.J., 1998. *An Introduction to Optical Dating*. Oxford University Press, Oxford.
- Alcaraz-Castaño, A. 2015. Central Iberia around the Last Glacial Maximum: Hopes and Prospects. *Journal of anthropological research* 71(4), 565-578
- Alcaraz-Castaño, M., Alcolea-González, J., Kehl, M., Albert, R.M., Baena-Preysler, J., de Balbín-Behrmann, R., Cuartero, F., et al., 2017. A context for the last Neanderthals of interior Iberia: Los Casares cave revisited. *PLoS ONE* 12, e0180823.
- Anderson, L., Chesnaux, L., Rué, M., Picavet, R., Fernandes, P., Morala, A., Caux, S., Tallet, P., Caverne, J.B., Kawalek, E., 2016. Regards croisés sur la station aurignacienne de Brignol (Villeneuve-sur-Lot, Lot-et-Garonne, France): approches

- taphonomique, pétroarchéologique, technoéconomique et technofonctionnelle de l'industrie lithique. *PALEO* 27, 11–42.
- Anderson, L., Reynolds, N., Teyssandier, N., 2019. No reliable evidence for a very early Aurignacian in Southern Iberia. *Nature Ecology and Evolution* 3, 713 doi:10.1038/s41559-019-0885-3.
- Angelucci, D.E., 2002. The Geoarchaeological Context. In: Zilhão, J., Trinkaus, E. (Eds.), *Portrait of the artist as a Child. The Gravettian Human Skeleton from the Abrigo do Lagar Velho and its Archaeological Context*. *Trabalhos de Arqueologia* 22, pp. 58–91.
- Angelucci, D.E., Anesin, D., Susini, D., Villaverde, V., Zapata, J., Zilhão, J., 2013. Formation processes at a high resolution middle Paleolithic site: Cueva Antón (Murcia, Spain). *Quaternary International* 315, 24–41.
- Aubry, T., 2009. 200 séculos da história do Vale do Côa: incursões na vida quotidiana do caçadores-artistas do Paleolítico. *Trabalhos de Arqueologia* 52.
- Aubry, T., Almeida, M., Neves, M.J., 2006. The Middle-to-Upper Palaeolithic transition in Portugal: An Aurignacian phase or not? Proceeding of the Symposium “Towards a definition of the Aurignacian”, Lisbon, Portugal. In: O. Bar-Yosef and J. Zilhão (eds.). *Trabalhos de Arqueologia* 45, pp. 95–108.
- Aubry, T., Dimuccio, L.A., Almeida, M., Neves, M.J., Angelucci, D., Cunha, L., 2011. Palaeoenvironmental forcing during the Middle-Upper Palaeolithic transition in Central-western Portugal. *Quaternary Research* 75, 66–79.
- Aubry, T., Dimuccio, L.A., Bergadá, M., Sampaio, J.D., Sellami, F., 2010. Palaeolithic engravings and sedimentary environments in the Côa River Valley (Portugal): Implications for the detection, interpretation and dating of open-air rock art. *Journal of Archaeological Science* 37, 3306–3319.
- Aubry, T., Gameiro, C., Santos, A.T., Luís, L., 2017. Existe Azilense em Portugal? Novos dados sobre o Tardiglacial e o Pré-Boreal no Vale do Côa. In Arnaud, J.M., Martins, A. (Eds.) *Arqueologia em Portugal 2017: Estado da Questão*. Lisboa: Associação dos Arqueólogos Portugueses, pp. 403–418.
- Aubry, T., Luís, L., Dimuccio, L.A., 2012a. Nature vs. Culture: present-day spatial distribution and preservation of open-air rock art in the Côa and Douro River Valleys (Portugal), *Journal of Archaeological Science* 39, 848–866.
- Aubry, T., Luís, L., Mangado Llach, J., Matias, H., 2012b. We will be known by the tracks we leave behind: exotic lithic raw materials, mobility and social networking among the Côa Valley foragers (Portugal). *Journal of Anthropological Archaeology* 31, 528–550.
- Aubry, T., Mangado Llach, X., Sellami, F., Sampaio, J.D., 2002. Open-air Rock-art. Territories and modes of exploitation during the Upper Paleolithic in the Côa Valley (Portugal). *Antiquity* 76, 62–76.
- Auclair, M., Lamothe, M., Huot, S., 2003. Measurement of anomalous fading for feldspar IRSL using SAR. *Radiation Measurements* 37, 487–492.
- Baena, J.P., Carrión, E., Torres, C.N., Vaquero, M.R., 2018. Mousterian inside the upper Paleolithic? The last interval of El Esquilieu (Cantabria, Spain) sequence. *Quaternary International*. <https://doi.org/10.1016/j.quaint.2018.11.015>.
- Banerjee, D., Murray, A.S., Bøtter-Jensen, L., Lang, A., 2001. Equivalent dose estimation using a single aliquot of polymineral fine grains. *Radiation Measurements* 33, 73–94.
- Bergadá, M.M., 2009. Análisis micromorfológico de la secuencia sedimentaria de Cardina I (Salto do Boi, Vila Nova de Foz Côa, Portugal). In Thierry Aubry (Ed.), 200 séculos da história do Vale do Côa: incursões na vida quotidiana do caçadores-artistas do Paleolítico. *Trabalhos de Arqueologia* 52, pp. 112–127.
- Bicho, N., Cascalheira, J., Gonçalves, C., 2017. Early Upper Paleolithic colonization across Europe: Time and mode of the Gravettian diffusion. *PLoS ONE* 12(5): e0178506. <https://doi.org/10.1371/journal.pone.0178506>.
- Blaauw, M., Christen, J.A., 2011. Flexible paleoclimate age-depth models using an autoregressive gamma process. *Bayesian Analysis* 6, 457–474.
- Boëda, E., 1993. Le débitage Discoïde et le débitage Levallois récurrent centripète. *Bulletin de la Société Préhistorique Française* 90, 392–404.
- Bøtter-Jensen, L., Thomsen, K.J., Jain, M., 2010. Review of optically stimulated luminescence (OSL) instrumental developments for retrospective dosimetry. *Radiation Measurements* 45, 253–257.
- Braga, M.A.S., Paquet, H., Begonha, A., 2002. Weathering of granites in a temperate climate (NW Portugal): granitic saprolites and arenization. *Catena* 49, 41–56.
- Bronger, A., Heinkele, T., 1990. Mineralogical and clay mineralogical aspects of loess research. *Quaternary International* 7–8, 37–51.
- Brown, A.G., 1997. *Alluvial geoarchaeology. Floodplain archaeology and environmental change*. Cambridge Manuals in Archaeology, University Press, New York.
- Buylaert, J.P., Jain, M., Murray, A.S., Thomsen, K.J., Thiel, C., Sotobatí, R., 2012. A robust feldspar luminescence dating method for Middle and Late Pleistocene sediments. *Boreas* 41, 435–451.
- Buylaert, J.P., Murray, A.S., Thomsen, K.J., Jain, M., 2009. Testing the potential of an elevated temperature IRSL signal from K-feldspar. *Radiation Measurements* 44, 560–565.
- Cardoso, J.L., 2006. O complexo mustierense em Portugal. *Zephyrus* 59, 21–50.
- Carrión, J.S., Fernández, S., Jiménez-Arenas, J.M., Munuera, M., Ochando, J., Amorós, G., Ponce de León, M., et al., 2019. The sequence at Carhuela Cave and its potential for research into Neanderthal ecology and the Mousterian in southern Spain. *Quaternary Science Reviews* 217, 194–216.
- Chamley, H., 1989. *Clay sedimentology*. Berlin, Springer Verlag.
- Cortés-Sánchez, M., 2007. *Cueva Bajondillo (Torremolinos). Secuencia cronocultural y paleoambiental del Cuaternario reciente de la Bahía de Málaga*. Centro de Ediciones de la Diputación Provincial de Málaga.
- Cortés-Sánchez, M., Jiménez-Espejo, F.J., Simón-Vallejo, M.D., Stringer, C., Francisco, M.C.L., García-Alix, A., Vera Peláez, J.L., et al., 2019. An early Aurignacian arrival in southwestern Europe. *Nature Ecology and Evolution*. doi.org/10.1038/s41559-018-0753-6.
- Cunha, P.P., Martins, A.A., Buylaert, J.P., Murray, A.S., Gouveia, M.P., Font, E., Pereira, T., et al., 2019. The Lowermost Tejo River Terrace at Foz do Enxarrique, Portugal: A Palaeoenvironmental Archive from c. 60–35 ka and Its Implications for the Last Neanderthals in Westernmost Iberia. *Quaternary* 2, 1–29.
- Cunha, P.P., Martins, A.A., Murray, A.S., Huot, S.; Raposo, L., 2008. Dating the Tejo river lower terraces in the Ródão area (Portugal) to assess the role of tectonics and uplift. *Geomorphology* 102, 43–54.
- Daura, J.J., Sanz, M., García, N., Allué, E., Vaquero, M., Fierro, E., Carrión, J.S., et al., 2012. Terrasses de la Riera dels Canyars (Gavà, Barcelona): the landscape of Heinrich Stadial 4 north of the “Ebro frontier” and implications for modern human dispersal into Iberia. *Quaternary Science Reviews* 60, 26–48.

- Davidson, I., 1986. The geographical study of Late Palaeolithic stages in Eastern Spain. In: G. Bailey and P. Callow (Eds.), *Stone Age Prehistory: Studies in Memory of Charles MacBurney*. Cambridge: Cambridge University Press, pp. 95–118.
- Demars, P.Y., Laurent, P., 1992. *Types d'outils lithiques du Paléolithique supérieur en Europe*. Cahiers du Quaternaire 14, CNRS édition.
- D'Errico, F., Sanchez-Goni, M.F., 2003. Neanderthal extinction and the millennial scale climatic variability of OIS 3. *Quaternary Science Reviews* 22, 769–788.
- Deschamps, M., Zilhão, J., 2018. Assessing site formation and assemblage integrity through stone tool refitting at Gruta da Oliveira (Almonda karst system, Torres Novas, Portugal): A Middle Paleolithic case study, *Plos One*, 13, 0192423.
- Devièse T., Karavanić, I., Comeskey, D., Kubiak, C., Korlević, P., Hajdinjak, M., Radović, S., et al., 2017. Direct dating of Neanderthal remains from the site of Vindija Cave and implications for the Middle to Upper Paleolithic transition. *Proceedings of the National Academy of Sciences* 114: 10606–10611.
- Dibble, H.L., Bar-Yosef, O. 1995. *The Definition and Interpretation of Levallois Technology*. Prehistory Press.
- Diekmann, B., Petschick, R., Gingele, F.X., Fütterer, D.K., Abelmann, A., Gersonde, R., Mackensen, A., 1996. Clay mineral fluctuations in Late Quaternary sediments of the southeastern South Atlantic: Implications for past changes of deep-water advection. In: Wefer, G., Berger, W.H., Siedler, G., Webb, D. (Eds.), *The South Atlantic: Present and Past Circulation*. Heidelberg, Springer, pp. 621–644.
- Esquevin, J., 1969. Influence de la composition chimique des Illites sur cristallinité. *Bulletin du Centre de Recherches de Pau* 3, 147–153.
- FAO-Isric, 1990. *Guidelines for soil description*. 3rd ed. FAO, Roma.
- Ferreira, A.B., 1978. *Planaltos e montanhas do norte da Beira*. Memórias do Centro de Estudos Geográficos 4, Lisbon.
- Finlayson, C., Pacheco, F.G., Rodríguez-Vidal, J., Fa, D.A., Gutierrez López, J.M., Santiago Pérez, A., Finlayson, G., et al., 2006. Late survival of Neandertals at the southernmost extreme of Europe. *Nature* 443, 850–853.
- Finlayson, C., Pacheco, F.G., Vidal, J.R., 2004. Did the moderns kill off the Neanderthals? A reply to F. d'Errico and Sánchez-Goni. *Quaternary Science Reviews* 23, 1205–1212.
- Fletcher, W., Sánchez-Goni, M.F., Allen, J.R.M., Cheddadi, R., Combourieu Nebout, N., Huntley, B., Lawson, I., et al., P.C., 2010. Millennial-scale variability during the last glacial in vegetation records from Europe. *Quaternary Sciences Reviews* 29, 2839–2864.
- Foucher, P., San-Juan-Foucher, C., Oberlin, C., 2011. Les niveaux d'occupation gravettiens de Gargas (Hautes-Pyrénées): Nouvelles données chronostratigraphiques. In: *A la recherche des identités gravettiennes: actualités, questionnements et perspectives*. Actes de la Table Ronde sur le Gravettien en France et dans les pays limitrophes, Aix-En-Provence, 6–8 octobre 2008. Mémoire LII de la Société Préhistorique Française, pp. 373–385.
- Galván, B., Hernández, C.M., Mallol, C., Mercier, N., Sistiaga, A., Soler, V., 2014. New evidence of early Neanderthal disappearance in the Iberian Peninsula. *Journal of Human Evolution* 75, 6–27.
- Gingele, F.X., 1996. Holocene climatic optimum in Southwest Africa—evidence from the marine clay mineral record. *Palaeogeography, Palaeoclimatology, Palaeoecology* 122, 77–87.
- Goldberg, P., Macphail, R.I., 2006. *Practical and theoretical geoarchaeology*. Blackwell Publishing. London.
- Guérin, G., Mercier, N., Adamiec, G., 2011. Dose-rate conversion factors: update. *Ancient TL* 29: 5–8.
- Higham, T., Douka, K., Wood, R., Bronk Ramsey, C., Brock, F., Basell, L., Camps, M., et al., 2014. The timing and spatiotemporal patterning of Neanderthal disappearance. *Nature* 512, 306–309.
- Higham, T.F.G., Jacobi, R.M., Basell, L., Bronk Ramsey, C., Chiotti, L., Nespoulet, R., 2011. Precision dating of the Palaeolithic: A new radiocarbon chronology for the Abri Pataud (France), a key Aurignacian sequence. *Journal of Human Evolution* 61, 549–563.
- Hofman, J.L., Enloe, J.G., 1992. *Piecing Together the Past: Application of Refitting Studies in Archaeology*. BAR International Series 578.
- Hublin, J.J., 2017. The last Neanderthal. *Proceedings of the National Academy of Sciences* 114: 10520–10522.
- Hublin, J.J., Barroso Ruiz, C., Medina Lara, P., Fontugne, M., Reys, J.L., 1995. The Mousterian site of Zafarraya (Andalucía, Spain): Dating and implication on the palaeolithic peopling process of western Europe. *Comptes Rendus de l'Académie des Sciences de Paris* 321 (IIa), 931–936.
- Huntley, D.J., Baril, M.R., 1997. The K content of the K-feldspars being measured in optical dating or in thermoluminescence dating. *Ancient TL* 15, 11–13.
- Jennings, R., Finlayson, C., Darren, F., Finlayson, G. 2011. Southern Iberia as a refuge for the last Neanderthal populations. *Journal of Biogeography* 38 (10), 1873–1885.
- Jiménez-Espejo, F.J., Rodríguez-Vidal, J., Finlayson, C., Martínez-Ruiz, F., Carrión, J.S., García-Alix, A., Paytan, A., et al., 2013. Environmental conditions and geomorphologic changes during the Middle-Upper Paleolithic in the southern Iberian Peninsula. *Geomorphology* 180–181, 205–216.
- Kahle, M., Kleber, M., Jahn, R., 2002. Review of XRD-based quantitative analyses of clay minerals in soils: the suitability of mineral intensity factors. *Geoderma* 109, 191–205.
- Keeley, H.C.M., Macphail, R.I. 1981. A Soil Handbook for Archaeologists. *Bulletin of the Institute of Archaeology London*, 225–243.
- Kehl, M., Burow, C., Hilgers, A., Navazo, M., Pastoors, A., Weniger, G.C., Wood, R., Jordá Pardo, J.F., 2013. Late Neanderthals at Jarama VI (Central Iberia)? *Quaternary Research* 80, 218–234.
- Keller, W.D., 1970. Environmental aspects of clay minerals. *Journal of Sedimentary Petrology* 40, 788–813.
- Klaric, L., 2015. Regional groups in the European Middle Gravettian: A reconsideration of the Rayssian technology. *Antiquity* 81, 176–190.
- Kübler, B., Jaboyedoff, M., 2000. Illite crystallinity. *Comptes Rendue de l'Académie des Sciences* 331, 75–89.
- Liu, X., Sun, Y., Vandenberghe, J., Li, Y., An, Z., 2018. Palaeoenvironmental implication of grain-size compositions of terrace deposits on the western Chinese Loess Plateau. *Aeolian Research* 32, 202–209.
- Mallol, C., Hernández, C.M., Machado, J., 2012. The significance of stratigraphic discontinuities in Iberian Middle-to-Upper Palaeolithic transitional sites. *Quaternary International* 275, 4–13.
- Mangado Llach, X., 2002. *La Caracterización y el Aprovechamiento de los Recursos Abióticos en la Prehistoria de Cataluña: Las Materias Primas Silíceas del Paleolítico Superior Final y el Epipaleolítico*. PhD dissertation, University of Barcelona.
- Marín-Arroyo, A.B., Rios-Garaizar J., Straus, L.G., Jones, J.R., de la Rasilla, M., González Morales, M.R., Manuel R., Richards, M., Altuna, J., Mariezkurrena, K., Ocio, D., 2018. Chronological reassessment of the Middle to Upper Paleolithic transition and Early

- Upper Paleolithic cultures in Cantabrian Spain. *PLoS ONE* 13, e0194708. <https://doi.org/10.1371/journal.pone.0194708>.
- Maroto, J., Vaquero, M., Arrizabalaga, A., Baena, J., Baquedano, E., Jordá, J.F.P., Brugués, R.J., et al., 2012. Current issues in late Middle Palaeolithic chronology: New assessments from Northern Iberia. *Quaternary International* 247, 15–25.
- Mercier, N., Valladas, H., Aubry, T., Zilhão, J., Jorons, J.L., Reyss, J.L., Sellami, F., 2006. Fariseu: first confirmed open-air paleolithic parietal art site in the Côa Valley (Portugal). *Antiquity* 80, 310. <http://antiquity.ac.uk/ProjGall/mercier/index.htm>.
- Michel, A., 2010. *L'Aurignacien récent (post-ancien) dans le Sud-Ouest de la France: variabilité des productions lithiques*. Révision taphonomique et techno-économique des sites de Caminade-Est, Abri Pataud, Roc-de-Combe, Le Flageolet I, La Ferrassie et Combemeneue. PhD dissertation, Bordeaux I University.
- Moore, D., Reynolds, R., 1997. *X-Ray-Diffraction and the Identification and Analysis of Clay Minerals*. Univsity Press, Oxford.
- Moore, R.C.A., 1949. Meaning of facies. In: Longwell, C.A.R. (Ed.), *Sedimentary Facies in Geological History*, vol. 39. *Geological Society of America Memoir*, 1–34.
- Morala, A., Lenoir, M., Turq, A., 2005. Production et utilisation de supports normalisés lamino-lamellaires dans la chaîne opératoire des grattoirs Caminade du site du Pigeonnier à Gensac (Gironde, France). In: *Actes du colloque, Productions lamellaires attribuées à L'Aurignacien: Chaînes opératoires et perspectives technoculturelles*, XIV^e Congrès de l'UISP, Liège 2–8 septembre 2001. *Archéologiques* 1, Luxembourg, pp. 257–271.
- Mourre V., 2003. Discoïde ou pas Discoïde? Réflexions sur la pertinence des critères techniques définissant le débitage Discoïde, in Peresani M. (Ed.), *Discoïd Lithic Technology—Advances and implications*, Oxford, BAR International Series 1120, pp. 1–18.
- Murray, A.S., Helsteld, L.M., Autzen, M., Jain, M., Buylaert, J.P., 2018. Measurement of natural radioactivity: Calibration and performance of a high-resolution gamma spectrometry facility. *Radiation Measurements* 120, 215–220.
- Murray, A.S., Marten, R., Johnston, A., Martin, P., 1987. Analysis for naturally occurring radionuclides at environmental concentrations by gamma spectrometry. *Journal of Radioanalytical and Nuclear Chemistry* 115, 263–288.
- Murray, A.S., Thomsen, K.J., Masuda, N., Buylaert, J.P., Jain, M., 2012. Identifying well-bleached quartz using the different bleaching rates of quartz and feldspar luminescence signals. *Radiation Measurements* 47, 688–696.
- Murray, A.S., Wintle, A.G., 2000. Luminescence dating of quartz using an improved single-aliquot regenerative-dose protocol. *Radiation Measurements* 32, 57–73.
- Murray, A.S., Wintle, A.G., 2003. The single aliquot regenerative dose protocol: potential for improvements in reliability. *Radiation Measurements* 37, 377–381.
- Paton, T.R., 1978. *The Formation of Soil Material*. George Allen and Unwin Press, London.
- Pe-Piper, G., Dolansky, L., Piper, D.J.W., 2005. Sedimentary environment and diagenesis of the Lower Cretaceous Chas-wood Formation, southeastern Canada: The origin of kaolin-rich mudstones. *Sedimentary Geology* 178, 75–97.
- Pelegrin, J., 1995. *Technologie lithique: le Châtelperronien de Roc-de-Combe (Lot) et de La Côte (Dordogne)*. Cahiers du Quaternaire 20, Editions CNRS, Paris.
- Peña Alonso, P., 2010. *Sobre la unidad tecnológica del Gravetiense en la Península Ibérica: implicaciones para el conocimiento del Paleolítico Superior inicial*. PhD dissertation, Universidad Complutense de Madrid.
- Peña Alonso, P., 2019. Dating on its own cannot resolve hominin occupation patterns. *Nature Ecology and Evolution* 3, 712. doi:10.1038/s41559-019-0886-2.
- Peña Alonso, P., Vega Toscano, G., 2013. The Early Upper Paleolithic puzzle in Mediterranean Iberia. *Quatär* 60, 85–106.
- Prescott, J.R., Hutton, J.T., 1994. Cosmic ray contributions to dose rates for luminescence and ESR dating: large depths and long-term variations. *Radiation Measurements* 23, 497–500.
- Qin, X., Cai, B., Liu, T., 2005. Loess record of the aerodynamic environment in the east Asia monsoon area since 60,000 years before present. *Journal of Geophysical Research: Solid Earth* 110, B01204.
- Raposo, L., 1995. Ambientes, territorios y subsistencia en el paleolítico medio de Portugal, *Complutum* 6, 57–75.
- Rasmussen, O., Bigler, M., Blockley, S.P., Blunier, T., Buchardt, S.L., Clausena, H.B., Cvijanovic, I., et al., 2014. A stratigraphic framework for abrupt climatic changes during the Last Glacial period based on three synchronized Greenland ice-core records: refining and extending the INTIMATE event stratigraphy. *Quaternary Science Review* 106, 14–28.
- Reimer, P.J., Bard, E., Bayliss, A., Beck, J.W., Blackwell, P.G., Bronk Ramsey, C., Buck, C.E., et al., 2013. IntCal13 and Marine13 radiocarbon age calibration curves, 0–50,000 years cal BP. *Radiocarbon* 55, 1869–1887.
- Ricci Lucchi, F., 1980. *Sedimentologia. Parte III. Ambienti Sedimentari e Facies*. Seconda edizione. CLUEB, Cooperativa Libreria Universitaria Editrice Bologna.
- Rigaud, J.Ph., 1982. *Le Paléolithique en Périgord: les données du Sud-Ouest sarladais et leurs implications*. PhD dissertation, Bordeaux I University, 2 vol.
- Rigaud, J.Ph., Simek, J., Delpech, F., Texier, J.P., 2016. The Aurignacian and Gravettian in northern Aquitaine: the contribution of Flageolet I. *PALEO*, 27, 265–295.
- Sepulchre, P., Ramstein, G., Kageyama, M., Vanhaeren, M., Krininger, G., Sánchez-Goñi, M.F., Errico, F., 2007. H4 abrupt event and late Neanderthal presence in Iberia. *Earth and Planetary Science Letters* 258 (1–2), 283–292.
- Silva, A.F., Ribeiro, M.L., 1991. Carta Geológica de Portugal em escala 1:50,000 e Notícia explicativa da Folha 15-A: Vila Nova de Foz Côa, Serviço Geológico de Portugal, Lisbon.
- Singer, A., 1980. The paleoclimatic interpretation of clay minerals in soils and weathering profiles. *Earth-Science Reviews* 15, 303–326.
- Singer, A., 1984. The paleoclimatic interpretation of clay minerals in sediments—a review. *Earth-Science Reviews* 21, 251–293.
- Sitzia, L., Bertran, P., Sima, A., Chery, P., Queffelec, A., Rousseau, D.D., 2017. Dynamics and sources of last glacial aeolian deposit in southwest France derived from dune patterns, grain-size gradients and geochemistry, and reconstruction of efficient wind directions. *Quaternary Science Review* 170, 250–268.
- Sonnevilles-Bordes, D. de, Mortureux, B., 1956. Outils aurignaciens nouveaux et rares. *L'Anthropologie*, 60, 574–578.
- Straus, L., Bicho, N., Winegardner, A., 2000. The Upper Paleolithic settlement of Iberia: first generation maps. *Antiquity* 74, 553–566.
- Sun, D., Bloemendal, J., Rea, D.K., Vandenberghe, J., Jiang, F., An, Z., Su, R., 2002. Grain-size distribution function of polymodal sediments in hydraulic and aeolian environments, and numerical partitioning of sedimentary components. *Sedimentary Geology* 152, 262–277.
- Thiébaud, C., 2007. Le Moustérien à denticulés des années 1950 à nos jours: définitions et caractérisation. *Bulletin de la Société Préhistorique Française* 104, 461–481.

- Thiel, C., Buylaert, J.P., Murray, A., Terhorst, B., Hofer, I., Tsukamoto, S., Frechen, M., 2011. Luminescence dating of the Stratzing loess profile (Austria) e testing the potential of an elevated temperature post-IR IRSL protocol. *Quat. Int.* 234, 23–31.
- Thomsen, K.J., Murray, A.S., Jain, M., Bøtter-Jensen, L., 2008. Laboratory fading rates of various luminescence signals from feldspar-rich sediment extracts. *Radiation Measurements* 43, 1474–1486.
- Torres, V., Vandenberghe, J., Hooghiemstra, H., 2005. An environmental reconstruction of the sediment infill of the Bogota basin (Columbia) during the last 3 million years from abiotic and biotic proxies. *Palaeogeography, Palaeoclimatology, Palaeoecology* 226, 127–148.
- Trinkaus, E., Maki, J., Zilhão, J., 2007. Middle Paleolithic Human Remains from the Gruta da Oliveira (Torres Novas), Portugal. *American Journal of Physical Anthropology* 134, 263–273.
- Valladas, H., Mercier, N., Froget, L., Jorons, J.L., Reyss, J.L., Aubry, T., 2001. TL Dating of Upper Paleolithic Sites in the Côa Valley (Portugal). *Quaternary Science Reviews* 20, 939–943.
- Villa, P., 1982. Conjoinable pieces and site formation processes. *American Antiquity* 47, 277–290.
- Villaverde, V., Real, C., Roman, D., Albert, R.M., Badal, E., Bel, M.A., Bergadá, M.M., *et al.*, 2019. The early Upper Palaeolithic of Cova de les Cendres (Alicante, Spain). *Quaternary International* 515, 92–124.
- Wolf, D., Kolb, T., Alcaraz-Castaño, M., Heinrich, S., Baumgart, P., Calvo, R., Sánchez, J., *et al.*, 2018. Climate deteriorations and Neanderthal demise in interior Iberia. *Nature*. Scientific Report 8, article 7048.
- Wolff, E.W., Chappellaz, J., Blunier, T., Rasmussen, S.O., Svensson, A., 2010. Millennial-scale variability during the last glacial: the ice core record. *Quaternary Science Reviews* 29, 2828–2838.
- Wood, R., Arrizabalaga, A., Camps, M., Fallon, S., Iriarte-Chiapusso, M.J., Jones, R., Maroto, J., *et al.*, 2014. The chronology of the earliest Upper Palaeolithic in northern Iberia: New insights from L'Arbreda, Labeko Koba and La Viña. *Journal of Human Evolution* 69, 91–109.
- Wood, R., Barroso-Ruíz, C., Caparrós, M., Jordá Pardo, J.F., Galván Santos, B., Higham, T., 2013. Radiocarbon dating casts doubt on the late chronology of the Middle to Upper Palaeolithic transition in southern Iberia. *Proceedings of the National Academy of Sciences* 110, 2781–2786.
- Xiao, J.L., Fan, J.W., Zhai, D.Y., Wen, R.L., Qin, X.G., 2015. Testing the model for linking grain-size component to lake level status of modern clastic lakes. *Quaternary International* 355, 34–43.
- Zilhão, J., 1997. *O Paleolítico Superior da Estremadura Portuguesa*, 2 Vols. Edições Colibri, Lisboa.
- Zilhão, J., 2006a. Chronostratigraphy of the Middle-to-Upper Paleolithic Transition in the Iberian Peninsula. *Pyrenae* 37, 7–84.
- Zilhão, J., 2006b. The Aurignacian of Portugal: a Reappraisal. In: Baquedano, E. Maíllo-Fernández, J.M. (Eds.), *Homenagem a Victória Cabrera. Zona Arqueológica* 7, Vol I, pp. 372–395.
- Zilhão, J. 2001. Middle Palaeolithic Settlement Patterns in Portugal. In: Conard, N. (Ed.), *Settlement Dynamics of the Middle Palaeolithic and Middle Stone Age*, Tübingen, Kerns Verlag, p. 597–608.
- Zilhão J., 2000. The Ebro Frontier: A model for the late extinction of Iberian neanderthals. In: Stringer, C.B., Barton, R.N., Finlayson, J.C. (Eds.), *Neanderthals on the Edge: Papers from a Conference Marking the 150th Anniversary of the Forbes' Quarry Discovery, Gibraltar*. Oxbow Books, Oxford, pp. 111–122.
- Zilhão, J., Ajas, A., Badal, E., Burrow, C., Kehl, M., López-Sáez, J. A., Pimenta, C., *et al.*, 2016. Cueva Antón: A multi-proxy MIS-3 to MIS-5: a paleoenvironmental record for SE Iberia. *Quaternary Science Reviews*, 146, 251–273.
- Zilhão, J., Anesin, D., Aubry T., Badal, E., Cabanes, D., Kehl, M., Klasen, N., *et al.*, 2017. Precise dating of Middle-to-Upper Palaeolithic transition in Murcia (Spain) supports late Neanderthal persistence in Iberia. *Helyion* (3).
- Zilhão, J.; Aubry, T.; Carvalho, A. M. F.; Zambujo, G., Almeida, F. 1995. O sítio arqueológico paleolítico do Salto do Boi (Cardina, Santa Comba, Vila Nova de Foz Côa), *Trabalhos de Antropologia e Etnologia* 35(4), pp. 471–485.
- Zilhão, J., Cardoso, J.L., Pike, A.W.G., Weninger, B., 2011. Gruta Nova da Columbeira (Bombarral, Portugal): Site stratigraphy, age of the Mousterian sequence, and implications for the timing of Neanderthal extinction in Iberia. *Quartär* 58, 93–112.
- Zilhão, J., Davis, S.J.M., Duarte, C., Soares, A.M.M., Steier, P., Wild, E., 2010. Pego do Diabo (Loures, Portugal): Dating the Emergence of Anatomical Modernity in Westernmost Eurasia. *PLoS ONE*, 5, 8880.
- Zilhão, J., Pettitt, P., 2006. On the new dates for Gorham's Cave and the late survival of Iberian Neanderthals. *Before Farming: The Archaeology and Anthropology of Hunter-Gatherers* 3, pp. 1–9.
- Zilhão, J., Trinkaus, E., 2002. (Eds.). *Portrait of the Artist as a Child. The Gravettian Human Skeleton from the Abrigo do Lagar Velho*. Lisboa, IPA, *Trabalhos de Arqueologia*, 22.